

K-inflationary Power Spectra in the Uniform Approximation

Larissa Lorenz* and Jérôme Martin†

*Institut d'Astrophysique de Paris, UMR 7095-CNRS,
Université Pierre et Marie Curie, 98bis boulevard Arago, 75014 Paris, France*

Christophe Ringeval‡

*Theoretical and Mathematical Physics Group, Centre for Particle Physics and Phenomenology,
Louvain University, 2 Chemin du Cyclotron, 1348 Louvain-la-Neuve, Belgium*

(Dated: January 7, 2009)

The advent of explicit Dirac–Born–Infeld (DBI) inflationary models within string theory has drawn renewed interest to the cosmological role of unusual scalar field dynamics, usually referred to as k-inflation. In this situation, the standard method used to determine the behavior of cosmological perturbations breaks down. We present a generic method, based on the uniform approximation, to analytically derive the power spectra of scalar and tensor perturbations. For this purpose, a simple hierarchy of parameters, related to the sound speed of the cosmological fluctuations and its successive derivatives, is introduced in a k-inflation analogue of the Hubble flow functions. The scalar spectral index and its running are obtained up to next to next to leading order for all k-inflationary models. This result relies on the existence of a well-motivated initial state, which is not trivial in the present context: having the wavelength of the Fourier mode smaller than the sonic horizon is indeed not enough and some conditions on the dynamics of the sound speed are also required. Our method is then applied to various models encountered in the literature. After deriving a generic slow-roll trajectory valid for any DBI model, simple formulae for the cosmological observables are obtained. In particular, the running, as the spectral index, for the so-called UV and IR brane inflationary models is found to be uniquely determined by the 't Hooft coupling. Finally, the accuracy of these cosmological predictions is assessed by comparing the analytical approximations with exact numerical integrations.

PACS numbers: 98.80.Cq, 98.70.Vc

I. INTRODUCTION

The primordial matter perturbations held responsible for growth and formation of large scale structure are commonly traced back to quantum fluctuations of a scalar field φ which should have dominated the energy density in the Universe at early times. The primordial power spectrum of both the scalar and tensor perturbations is a calculational output of the inflationary scenario, and the recent Cosmic Microwave Background (CMB) experiments have gathered considerable evidence in favor of it [1, 2, 3, 4, 5, 6].

A compelling virtue of the inflationary paradigm is the fact that it can be sustained by a whole class of scalar field potentials $V(\varphi)$, provided these exhibit characteristics (*i.e.* in their slope and curvature) in agreement with the “slow-roll” conditions: while inflation is under way, the potential must dominate over the kinetic energy $\dot{\varphi}^2/2$, that is, $\ln V$ should be flat enough not to accelerate the field quickly. The slow-roll regime for inflation is described by a hierarchy of parameters ϵ_i , assumed to be small, in which the primordial power spectra can be analytically expressed as a Taylor expansion

[7, 8, 9, 10, 11, 12].

A large body of literature is devoted to the search for inflationary scenarios, in the sense that they should be naturally motivated by a high energy physics theory [13]. For example, the toolkit of ten-dimensional super-string theory and its various compactifications to an effective four-dimensional field theory has been used to design candidate potentials [14, 15, 16].

An interesting approach studies the effect of modifications to the kinetic term of the inflaton (k-inflation) [17]; in the perturbation treatment, these modifications manifest themselves as a (possibly time-dependent) “speed of sound” $c_s \neq 1$ (the speed of light being $c = 1$) for the scalar Fourier modes [18]. It turns out that string inflation models where the inflaton field is an open string mode are typically of this kind, with the speed of sound being a function of the background geometry [19, 20]. Hence inflationary model building in string theory combines both candidate potentials and non-canonical field evolution.

The prime example of these scenarios are the so-called brane inflation models, where the inflaton φ corresponds to the position of a D -brane within a higher-dimensional manifold [21, 22, 23]. Being an open string mode, φ has a Dirac–Born–Infeld (DBI) action, which is essentially the square root of the induced metric on the brane. This metric, in turn, contains information about the chosen background compactification of the extra-dimensions through the position-dependent brane ten-

*Electronic address: lorenz@iap.fr

†Electronic address: jmartin@iap.fr

‡Electronic address: christophe.ringeval@uclouvain.be

sion $T(\varphi)$. The inflaton potential $V(\varphi)$ can be of various shape, and its exact calculation remains a matter of active research [24, 25]. Typically, it receives contributions involving $T(\varphi)$, but may also be affected by finer geometric detail such as the presence of other branes in the extra-dimensional background geometry. As a natural consequence of the non-canonical interplay between potential and dynamics in the k-inflation case, one can no longer trust the intuition that flat potentials support inflation. Through $T(\varphi)$, the warping of the background acts as a break on the field, allowing potential energy domination and accelerated expansion of the Universe even when $\ln V$ is steep.

As it is clear from the above description, the standard methods of slow-roll inflation break down in the case of k-inflation. In particular, the formula expressing the background trajectory is modified since the shape of $T(\varphi)$ (and not only the shape of the potential as in the ordinary case) affects the motion of the mobile brane. Another new feature of k-inflation, which is of prime concern for this article, is that one can no longer calculate the cosmological perturbations' power spectra using the standard techniques. Indeed, as already mentioned above, the scalar perturbations have now a time-dependent speed of propagation which prevents us to integrate the equations of motion in terms of Bessel functions. Moreover, concerning the perturbations' evolution, the "usual" Hubble flow functions ϵ_i do no longer provide a sufficient description. Therefore, the main goal of this paper is to put forward a general formalism for k-inflation, resembling as far as possible the usual slow-roll formalism, where all these issues can be addressed in a consistent and unified way.

The paper is organized as follows. In Sec. II, we use a combined hierarchy (ϵ_i, δ_i) of Hubble and "sound" flow functions such that $\epsilon_i, \delta_i \ll 1, i \geq 1$ is the analogue of the standard slow-roll approximation [20, 26, 27, 28]. Then, using the background equations of motion, the slow-roll trajectory is expressed as a quadrature. Our new formula can be applied to any DBI model (but not to k-inflationary models in general) characterized by the functions $T(\varphi)$ and $V(\varphi)$ and is valid under a single assumption, namely $\epsilon_1 \ll 1$. In a next step, we carry on through the calculation of the k-inflationary perturbation spectra in full generality (but assuming, as usual, the smallness of the Hubble and sound flow parameters), including the non-trivial effects induced by a varying sound speed, in the so-called uniform approximation [29, 30]. In particular, we derive the scalar spectral index and the running at the next to next to leading order for a general model of k-inflation. Moreover, we show that a time-dependent sound horizon may lead to sub-sonic Fourier modes starting their evolution out of the Wentzel-Kramers-Brillouin (WKB) regime. This generically results in oscillations in the primordial scalar power spectrum. At the end of this section, we also discuss how the new parameters can be used to generalize to k-inflation the classification of (single field) inflationary models described in Ref. [12]. Then,

in Sec. III, our approach is applied to various example models encountered in the literature. In particular, we recover or extend previous results concerning power-law DBI inflation [31, 32], the Kachru–Kallosh–Linde–Maldacena–McAllister–Trivedi (KKLMMT) model [19], chaotic Klebanov–Strassler (CKS) inflation [28, 33, 34], and derive new results for models having a CKS potential plus constant [35]. At various stages, we assess the accuracy of our approximation scheme from exact numerical integrations. In Sec. IV, we recap and discuss our main findings. Finally, in three short appendices, we briefly compare our new hierarchy of parameters to the parameters already considered before in the literature and we recall how the master equation for the Mukhanov-Sasaki variable can be derived in k-inflation.

II. DBI SLOW-ROLL INFLATION

In this section, although we are concerned with the DBI models, the definition of the Hubble and sound flow parameters is valid in full generality for all k-inflationary models [17]. The same remark holds for the calculation of the primordial power spectra and will be made apparent by using explicitly the sound speed c_s in the calculations.

A. Basic equations

The basic construction behind brane inflation models in super-string theory is discussed in several recent reviews [14, 16, 36, 37]. Our starting point is the effective four-dimensional inflaton action

$$S = - \int d^4x \sqrt{-g} \left[T(\varphi) \sqrt{1 + \frac{1}{T(\varphi)} g^{\mu\nu} \partial_\mu \varphi \partial_\nu \varphi} + V(\varphi) - T(\varphi) \right], \quad (1)$$

with $V(\varphi)$ the potential and $T(\varphi)$ the warp function. The warp function is determined by a specific choice for the geometry of the extra-dimensions. The shape of the potential receives many different contributions, which include Coulomb-like terms describing the attraction between branes and anti-branes as well as terms that arise from the embedding of different dimensional branes. On the string theory side, there is an ongoing debate on the number and form of these contributions. The form of $T(\varphi)$ is the subject of less controversy since known string inflation models use the singular conifold or its cousin, the deformed conifold [33]. However, $T(\varphi)$ has also been treated as a completely general function in the literature, and here, both $V(\varphi)$ and $T(\varphi)$ will be considered as free functions in the sake of generality.

It is worth noticing that the action (1) defines a consistent theory. Indeed, for an arbitrary model of k-inflation,

the action of the scalar field can be written as

$$S_k = \int d^4x \sqrt{-g} P(X, \varphi), \quad (2)$$

where the quantity $X \equiv -(1/2)g^{\mu\nu}\partial_\mu\varphi\partial_\nu\varphi$. One can show [38] that this theory is well-defined if

$$\frac{\partial P}{\partial X} > 0, \quad 2X \frac{\partial^2 P}{\partial X^2} + \frac{\partial P}{\partial X} > 0. \quad (3)$$

The first condition comes from the requirement that the Hamiltonian should be bounded from below while the second is necessary if one wants the field equations to remain hyperbolic [38]. In the case of DBI, one has $P = -T\sqrt{1 - 2X/T}$ and one can check that both conditions are indeed satisfied regardless of the sign of the brane tension $T(\varphi)$. In the following, we will always restrict ourselves to models of k-inflation that fulfill the above-mentioned conditions.

Variation of Eq. (1) with respect to the metric gives the DBI stress-energy tensor,

$$T_{\mu\nu} = -\frac{2}{\sqrt{-g}} \frac{\delta S}{\delta g^{\mu\nu}}. \quad (4)$$

which is found to read

$$T_{\mu\nu} = \gamma \partial_\mu \varphi \partial_\nu \varphi - g_{\mu\nu} \left[V(\varphi) + T(\varphi) \left(\frac{1}{\gamma} - 1 \right) \right], \quad (5)$$

where the Lorentz factor is defined as [20, 39]

$$\gamma \equiv \left[1 + \frac{1}{T(\varphi)} g^{\alpha\beta} \partial_\alpha \varphi \partial_\beta \varphi \right]^{-1/2}. \quad (6)$$

The relativistic analogy becomes evident in the case where one considers a spatially homogeneous field $\varphi(t)$ in a Friedmann–Lemaître–Robertson–Walker (FLRW) universe so that Eq. (6) simplifies to

$$\gamma = \frac{1}{\sqrt{1 - \dot{\varphi}^2/T(\varphi)}}, \quad (7)$$

where a dot denotes a derivative with respect to cosmic time. Clearly, $\sqrt{T(\varphi)}$ here plays the role of an upper limit on the inflaton's velocity $\dot{\varphi}$. When expanding γ for $\dot{\varphi}^2 \ll T(\varphi)$, the action at first order resumes its canonical form. Moreover, the energy density and pressure read

$$\rho = (\gamma - 1)T(\varphi) + V(\varphi), \quad p = \frac{\gamma - 1}{\gamma} T(\varphi) - V(\varphi), \quad (8)$$

so that we have the Friedmann–Lemaître equations

$$H^2 = \frac{\kappa}{3} [(\gamma - 1)T + V], \quad (9)$$

$$2\dot{H} + 3H^2 = \kappa \left(\frac{1 - \gamma}{\gamma} T + V \right), \quad (10)$$

while the Klein-Gordon equation for the field reads

$$\ddot{\varphi} + \frac{3H}{\gamma^2} \dot{\varphi} + \frac{3\gamma - \gamma^3 - 2}{2\gamma^3} \frac{dT}{d\varphi} + \frac{1}{\gamma^3} \frac{dV}{d\varphi} = 0. \quad (11)$$

The constant κ is defined by $\kappa \equiv 8\pi/m_{\text{Pl}}^2$, m_{Pl} being the four-dimensional Planck mass.

B. DBI slow-roll trajectory

In standard inflation, one usually defines a hierarchy of Hubble flow parameters from [10, 11, 12]

$$\epsilon_{n+1} = \frac{d \ln |\epsilon_n|}{dN}, \quad \epsilon_0 \equiv \frac{H_{\text{in}}}{H}. \quad (12)$$

Their physical interpretation is that the expansion is accelerated as long as $\epsilon_1 < 1$ (potential energy domination). The slow-roll approximation assumes moreover that one has $|\epsilon_i| \ll 1$, $i \geq 1$, a condition which is in general necessary in order to have a sufficient number of e-folds. In addition, this last condition also allows us to integrate analytically the field trajectory and to compute the cosmological perturbations' power spectra.

In DBI inflation, we still retain the definition (12), the only subtlety being that the Hubble parameter is now given by Eqs. (9) and (10). Expressed in terms of derivatives of H with respect to φ , the first two Hubble flow functions read

$$\epsilon_1 = \frac{2}{\kappa\gamma} \frac{1}{H^2} \left(\frac{dH}{d\varphi} \right)^2, \quad (13)$$

$$\epsilon_2 = \frac{2}{\kappa\gamma} \left[\frac{2}{H^2} \left(\frac{dH}{d\varphi} \right)^2 - \frac{2}{H} \frac{d^2 H}{d\varphi^2} + \frac{1}{\gamma} \frac{d\gamma}{d\varphi} \frac{1}{H} \frac{dH}{d\varphi} \right]. \quad (14)$$

In comparison with the standard case, we see that the expression of ϵ_1 contains a γ factor in the denominator. This merely expresses the fact that, even if the potential is not flat, inflation may occur provided $\gamma \gg 1$. Let us also recall that the above definition is fact valid for any k-inflation model with the replacement $\gamma = 1/c_s$.

In fact, one does not need more to derive the slow-roll trajectory for any DBI model. Let us first notice that Eq. (7) can be recast into

$$\left(\frac{dN}{d\varphi} \right)^2 = \frac{\gamma^2 H^2}{(\gamma^2 - 1)T}. \quad (15)$$

The Lorentz factor γ can now be expressed exclusively in terms of H and φ . Indeed, Eq. (10) together with $\dot{H} = \dot{\varphi} dH/d\varphi$ yields

$$\dot{\varphi} = -\frac{2}{\kappa\gamma} \frac{dH}{d\varphi}, \quad (16)$$

which can be used to replace $\dot{\varphi}$ in Eq. (7). Solving for γ leads to

$$\gamma(\varphi) = \sqrt{1 + \frac{4}{\kappa^2 T} \left(\frac{dH}{d\varphi} \right)^2}. \quad (17)$$

Therefore, despite the fact that γ contains a $\dot{\varphi}$ factor, it can be viewed as a function of the inflaton field only. Moreover, as shown in Ref. [40], Eq. (9) can be recast as

$$3H^2 = \frac{\kappa V}{1 - \frac{2\gamma}{3(\gamma + 1)} \epsilon_1}. \quad (18)$$

Let us notice that, up to this point, all equations are exact. To proceed further, we use the slow-roll approximation to simplify Eq. (18) by assuming $\epsilon_1 \ll 1$. In this limit, since $\gamma \geq 1$, one has

$$H^2 \simeq \frac{1}{3} \kappa V. \quad (19)$$

The DBI analogue to the standard slow-roll trajectory is readily obtained by replacing γ in Eq. (15) from its expression (17) and using Eq. (19) for the Hubble parameter,

$$N(\varphi) = \mp \kappa \int_{\varphi_{\text{ini}}}^{\varphi} \sqrt{\left(\frac{V}{V_{,\psi}}\right)^2 + \frac{1}{3} \frac{V}{\kappa T}} d\psi. \quad (20)$$

As a result, only the knowledge of V and T is required to calculate the DBI slow-roll trajectory, just as knowing the potential accomplishes the same goal in the standard case. Let us mention again that the only assumption that goes into obtaining Eq. (20) is $\epsilon_1 \ll 1$. As we will see in the next section, additional approximations are nevertheless required at the perturbative level.

The new degrees of freedom introduced by the warp function $T(\varphi)$ suggest to define an additional hierarchy of parameters [26, 41]. In fact, in the same way that the ϵ_i encode the Hubble parameter evolution, it is convenient to consider their equivalent in terms of the “sound horizon”. Therefore, we define the δ_i , the sound flow functions, in a way similar to the Hubble flow parameters, but starting with the sound speed c_s :

$$\delta_{n+1} = \frac{d \ln |\delta_n|}{dN}, \quad \delta_0 \equiv \frac{c_{s \text{ in}}}{c_s}. \quad (21)$$

In the case of DBI inflation, one gets for the two first parameters

$$\delta_1 = -\frac{2}{\kappa \gamma} \frac{1}{\gamma} \frac{d\gamma}{d\varphi} \frac{1}{H} \frac{dH}{d\varphi}, \quad (22)$$

$$\delta_2 = \frac{2}{\kappa \gamma} \left[\frac{2}{\gamma} \frac{d\gamma}{d\varphi} \frac{1}{H} \frac{dH}{d\varphi} - \frac{d^2 \gamma / d\varphi^2}{d\gamma / d\varphi} \frac{1}{H} \frac{dH}{d\varphi} + \frac{1}{H^2} \left(\frac{dH}{d\varphi} \right)^2 - \frac{1}{H} \frac{d^2 H}{d\varphi^2} \right]. \quad (23)$$

The full hierarchy is therefore given by the combined set (ϵ_i, δ_i) . Let us notice that, as in standard inflation, it is also possible to introduce various sets of flow parameters and one could also have a set of potential and warp function based parameters. Such an alternative hierarchy (ϵ_v, ϵ_T) is summarized in the Appendix A for completeness. Finally, the ϵ_i and δ_i defined here correspond to a subset of the “brane inflation flow functions” previously defined in Refs. [27, 34, 35].

C. K-inflationary perturbations

In this subsection, we now turn to the theory of cosmological perturbations in k-inflation.

1. Equation of motion for the scalar modes

The main gauge-invariant equations for the cosmological perturbations are reviewed in Appendix C. There, it was shown that the (Fourier amplitude of the) Mukhanov-Sasaki variable obeys the following equation [18]

$$v_{\mathbf{k}}'' + \left(c_s^2 k^2 - \frac{z''}{z} \right) v_{\mathbf{k}} = 0, \quad (24)$$

where a prime denotes a derivative with respect to conformal time and where the function z is given by the following expression:

$$z \equiv \frac{a\varphi'}{\mathcal{H}} \left(\frac{1}{c_s} \right)^{3/2} = \sqrt{\frac{2}{\kappa}} \frac{a}{c_s} \sqrt{\epsilon_1}. \quad (25)$$

As in the standard case, one obtains the equation of a parametric oscillator. However, there is an important twist: the sound speed c_s is no longer equal to unity but is now a time-dependent quantity which prevents the use of standard techniques to find solutions of this equation. In the DBI case, it is given by $c_s = 1/\gamma \leq 1$ and can take very low values.

As in the standard case, one can entirely express the effective potential in Eq. (24) in terms of the Hubble and sound flow functions,

$$\begin{aligned} \frac{(a\sqrt{\epsilon_1}/c_s)''}{(a\sqrt{\epsilon_1}/c_s)} = \mathcal{H}^2 \left[2 - \epsilon_1 + \frac{3}{2}\epsilon_2 + \frac{1}{4}\epsilon_2^2 - \frac{1}{2}\epsilon_1\epsilon_2 + \frac{1}{2}\epsilon_2\epsilon_3 \right. \\ \left. + (3 - \epsilon_1 + \epsilon_2)\delta_1 + \delta_1^2 + \delta_1\delta_2 \right]. \end{aligned} \quad (26)$$

As expected, there are additional terms proportional to the sound flow parameters.

As usual, the final goal is to compute the two-point correlation function or, in Fourier space, the power spectrum. For the scalar modes, its expression reads

$$\mathcal{P}_\zeta \equiv \frac{k^3}{2\pi^2} |\zeta_{\mathbf{k}}|^2 = \frac{k^3}{4\pi^2} \frac{c_s^2 \kappa |v_{\mathbf{k}}|^2}{a^2 \epsilon_1}, \quad (27)$$

where $\zeta_{\mathbf{k}} = v_{\mathbf{k}}/z$ is the comoving curvature perturbation. In order to estimate this quantity, one has to integrate the equation of motion (24) from a set of initial conditions over the background solution, given by Eq. (20) for the DBI models. We now turn to the question of the initial conditions.

2. Initial conditions

The effective time-dependent frequency of Eq. (24) is given by

$$\omega^2(k, \eta) = c_s^2 k^2 - \frac{(a\sqrt{\epsilon_1}/c_s)''}{(a\sqrt{\epsilon_1}/c_s)}. \quad (28)$$

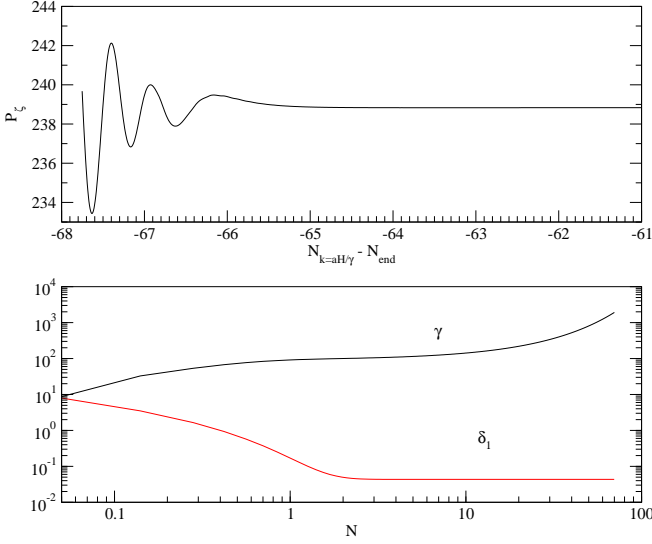


FIG. 1: Scalar power spectrum as a function of the number of e-folds N_k at which a given mode k crossed the sound horizon in the case of the chaotic Klebanov–Strassler model (see Sect. III B 2). The oscillations on large scales come from the violation of the WKB condition while the initial state is enforced to be a Bunch–Davies vacuum. The bottom panel shows the sound flow parameters as a function of the number of e-folds: $\delta_1 \gg 1$ initially triggers the WKB violation.

A well-defined and well-motivated initial state can be chosen in the adiabatic regime for which a WKB solution exists, i.e. for

$$\left| \frac{Q}{\omega^2} \right| \ll 1, \quad (29)$$

where the quantity Q is

$$Q(k, \eta) \equiv \frac{3}{4} \frac{\omega'^2}{\omega^2} - \frac{\omega''}{2\omega}. \quad (30)$$

In the standard case, the modes of astrophysical interest today are, at the beginning of inflation, such that their wavelength is smaller than the Hubble radius. This implies that $\omega \sim k$ and the quantity Q vanishes. As a consequence, the condition $|Q/\omega^2| \ll 1$ is obviously satisfied and the WKB state

$$v_{\mathbf{k}}(\eta) = \frac{\exp \left[i \int_{\eta_{\text{ini}}}^{\eta} \omega(k, \tau) d\tau \right]}{\sqrt{2\omega(k, \eta)}} \simeq \frac{1}{\sqrt{2k}} e^{ik(\eta - \eta_{\text{ini}})}, \quad (31)$$

is the preferred initial state.

However, in the k-inflationary case, the time-dependence of the sound speed brings new complications into this question [18, 20, 27, 42]. Indeed, even if initially, the modes are within the sound horizon and such that $\omega \sim c_s k$, the effective frequency is still a time-dependent quantity and, therefore, it is *a priori* not obvious that a well-defined state can be chosen in this context. One

has to check for each mode that the quantity Q/ω^2 is indeed small. From Eqs. (28) and (30), this one can be expressed in terms of the sound flow functions and reads

$$\frac{Q}{\omega^2} = \frac{a^2 H^2}{2c_s^2 k^2} \left(\delta_1 - \epsilon_1 \delta_1 + \delta_1 \delta_2 + \frac{1}{2} \delta_1^2 \right). \quad (32)$$

Assuming the slow-roll conditions on the ϵ_i are satisfied, the WKB condition (29) can still be violated as soon as $c_s k/\mathcal{H} \simeq \delta_1$, and thus even for the modes deep inside the sound horizon provided δ_1 is big enough. As an example of such a situation, Fig. 1 shows the scalar power spectrum obtained from a numerical integration of Eq. (24) in a case where $\delta_1 \gg 1$ initially, the warp function and potential being those of the chaotic Klebanov–Strassler model, see Sect. III B 2. Enforcing the modes to start in the Bunch–Davies vacuum is no longer justified and leads to oscillations in the power spectrum. Clearly, such a situation essentially concerns the modes crossing the sound horizon soon after the beginning of inflation, the ones for which $c_s k/\mathcal{H}$ cannot be chosen big enough to satisfy Eq. (29).

The conclusion is that, in order to be able to choose a well-motivated initial state for a given Fourier mode in k-inflation, it is not enough to have a wavelength smaller than the sound horizon. Additional conditions on the sound flow parameters δ_1 and δ_2 are also necessary. As shown before, a situation where $\lambda_k = 2\pi a/k$ is smaller than the sound horizon and $Q/\omega^2 \gg 1$ can easily be designed. In such a case, our ability to work with a well-defined initial state is lost.

D. The uniform approximation

At first order in the Hubble and sound flow functions, one can use the uniform approximation to solve the mode equation. The uniform approximation was developed in Refs. [29, 30]. For this purpose, it is convenient to rewrite Eq. (24) as

$$v_{\mathbf{k}}'' + \left(c_s^2 k^2 - \frac{\nu^2 - 1/4}{\eta^2} \right) v_{\mathbf{k}} = 0, \quad (33)$$

where the function $\nu(\eta)$ can be calculated from the effective potential given in Eq. (26). Following Refs. [29, 30], one also defines the two following functions:

$$g(\eta) \equiv \frac{\nu^2}{\eta^2} - c_s^2 k^2, \quad q(\eta) \equiv -\frac{1}{4\eta^2}. \quad (34)$$

The so-called turning point is defined by the condition $g(\eta_*) = 0$ and, for each mode, occurs at the time $\eta_*(k)$ such that

$$k\eta_* = -\frac{\nu_*}{c_{s*}}. \quad (35)$$

The uniform approximation tells us that the Mukhanov variable $v_{\mathbf{k}}$ can be expressed as [29, 30]

$$v_{\mathbf{k}}(\eta) = A_{\mathbf{k}} \left(\frac{f}{g} \right)^{1/4} \text{Ai}(f) + B_{\mathbf{k}} \left(\frac{f}{g} \right)^{1/4} \text{Bi}(f), \quad (36)$$

where $A_{\mathbf{k}}$ and $B_{\mathbf{k}}$ are two constants to be determined from the initial conditions and $\text{Ai}(x)$ and $\text{Bi}(x)$ denote the Airy functions of first and second kind respectively. The function $f(k, \eta)$ is defined by

$$f(k, \eta) = \frac{|\eta - \eta_*|}{\eta - \eta_*} \left| \frac{3}{2} \int_{\eta_*}^{\eta} d\tau \sqrt{|g(\tau)|} \right|^{2/3}. \quad (37)$$

As already discussed above, we assume that adiabaticity is valid initially, then choosing the initial conditions as an initial state of the WKB form yields

$$A_{\mathbf{k}} = iB_{\mathbf{k}}, \quad B_{\mathbf{k}} = \sqrt{\frac{\pi}{2}} e^{i\theta}, \quad (38)$$

where θ is just an unimportant scale-independent phase factor that will be ignored in the following. The solution (36) is now completely specified.

After the turning point, using the asymptotic behavior of the Airy functions, the solution can be written as

$$v_{\mathbf{k}}(\eta) \simeq \frac{B_{\mathbf{k}}}{g^{1/4} \pi^{1/2}} \exp\left(\frac{2}{3} f^{3/2}\right), \quad (39)$$

and one still has to calculate the integral in Eq. (37). For $\eta > \eta_*$, it simplifies to

$$\frac{2}{3} f^{3/2}(k, \eta) = \int_{\eta_*}^{\eta} d\tau \sqrt{\frac{\nu^2}{\tau^2} - c_s^2 k^2}. \quad (40)$$

The functions $\nu(\eta)$ and $1/c_s(\eta)$ can be expanded in terms of the Hubble and sound flow functions. For instance, assuming that $1/c_s$ admits a polynomial expansion around η_* , one has

$$\frac{1}{c_s(\eta)} = \sum_{n=0}^{\infty} \left(\frac{1}{c_s} \right)_{\eta_*}^{(n)} \frac{(\eta - \eta_*)^n}{n!}. \quad (41)$$

At first order, one finds from Eqs. (12) and (21)

$$\left(\frac{1}{c_s} \right)^{(n)} = \frac{1}{c_s} (n-1)! \mathcal{H}^n + \mathcal{O}(\epsilon\delta), \quad (42)$$

where $\mathcal{O}(\epsilon\delta)$ stands for all terms of order two in the ϵ_i , δ_i or mixed. Let us notice that all terms in Eq. (41) should be considered at first order in ϵ_i and δ_i . Plugging Eq. (42) into Eq. (41) yields an infinite sum that can however be resummed into

$$\frac{c_{s*}}{c_s(\eta)} = 1 - \delta_{1*} \ln[1 - \mathcal{H}_*(\eta - \eta_*)], \quad (43)$$

a star indicating that the corresponding quantity is evaluated at the turning point defined above. For consistency, \mathcal{H}_* has still to be expanded. Using

$$\mathcal{H}(\eta) = -\frac{1 + \epsilon_1}{\eta} + \mathcal{O}(\epsilon\delta), \quad (44)$$

one finally gets

$$\frac{1}{c_s(\eta)} = \frac{1}{c_{s*}} \left(1 - \delta_{1*} \ln \frac{\eta}{\eta_*} \right) + \mathcal{O}(\epsilon\delta). \quad (45)$$

Along the same line of reasoning, one would show that the function $\nu(\eta)$ reads

$$\nu^2(\eta) = \frac{9}{4} + 3\epsilon_{1*} + \frac{3}{2}\epsilon_{2*} + 3\delta_{1*} + \mathcal{O}(\epsilon\delta) = \nu_*^2 + \mathcal{O}(\epsilon\delta). \quad (46)$$

One can check that this expression matches with the standard result by setting $\delta_{1*} = 0$ (see Ref. [7]). Let us notice that one may avoid the infinite re-summation by performing an expansion directly in terms of the number of e-folds. Indeed, a Taylor expansion of $1/c_s(N)$ is also a flow expansion. For instance, one has

$$\frac{1}{c_s(N)} = \frac{1}{c_{s*}} + \frac{1}{c_{s*}} \delta_{1*} (N - N_*) + \mathcal{O}(\delta^2). \quad (47)$$

To recover the conformal time dependency one may use Eq. (44) to get

$$N - N_* = \ln \frac{a}{a_*} \simeq \ln \frac{(-\eta)^{-1-\epsilon_1}}{(-\eta_*)^{-1-\epsilon_{1*}}} = \ln \frac{\eta_*}{\eta} + \mathcal{O}(\epsilon). \quad (48)$$

Plugging the previous equation into Eq. (47) immediately gives Eq. (45).

Let us now return to the calculation of the function $f(k, \eta)$. Inserting Eqs. (45) and (46) into the integral (40), and defining the new variable

$$w \equiv \frac{c_{s*} k \eta}{\nu_*}, \quad (49)$$

one obtains at first order in the Hubble and sound flow parameters

$$\begin{aligned} \frac{2}{3} f^{3/2}(w) = & \left(-\frac{3}{2} - \epsilon_{1*} - \frac{1}{2}\epsilon_{2*} + \frac{1}{2}\delta_{1*} \right) \\ & \times \left(\sqrt{1-w^2} + \ln \frac{-w}{1+\sqrt{1-w^2}} \right) \\ & - \frac{3}{2} \delta_{1*} \sqrt{1-w^2} \ln(-w). \end{aligned} \quad (50)$$

where we have used Eq. (35). This expression will be used in the following to derive the power spectra.

E. Power spectra and spectral index

1. Scalar power spectrum

We are now in a position to estimate the power spectrum of scalar perturbations. The comoving curvature perturbation being constant on super-sonic length scales, see Appendix C, the power spectrum is obtained from Eq. (27), using Eqs. (39) and (50) in the limit $w \rightarrow 0$. Lengthy but straightforward calculations give, at first order in the Hubble and sound flow functions,

$$\begin{aligned} \mathcal{P}_{\zeta} = & \frac{H_*^2}{\pi m_{\text{Pl}}^2 \epsilon_{1*} c_{s*}} (18e^{-3}) \left[1 - 2 \left(\frac{4}{3} - \ln 2 \right) \epsilon_{1*} \right. \\ & \left. - \left(\frac{1}{3} - \ln 2 \right) \epsilon_{2*} + \left(\frac{7}{3} - \ln 2 \right) \delta_{1*} \right]. \end{aligned} \quad (51)$$

Notice that the above expression is still an implicit function of k through its dependence on η_* . Let us also remark the presence of the factor $18e^{-3} \sim 0.896$ in the overall amplitude, which is typical for the WKB and uniform approximations. As discussed in Ref. [43], this is rather unfortunate since this factor damages the approximation of the overall amplitude down to the 10% level. However, as shown for instance in Ref. [44], this problem can be rather easily fixed. Very roughly, one can renormalize $18e^{-3}$ to one to recover the exact amplitude [43]. The spectral index is, on the contrary, predicted accurately by the WKB and uniform approximations.

To remove the implicit dependence in k hidden in η_* , we define a pivot wavenumber k_\diamond and expand all terms around an unique conformal time η_\diamond which is the time when the pivot scale crossed the “sound horizon”, namely

$$-k_\diamond \eta_\diamond = \frac{1}{c_{s\diamond}}. \quad (52)$$

Then, one can use the flow expansions for \mathcal{H} , $1/c_s$, and the ϵ_i , δ_i , but now around η_\diamond . In this case, Eq. (51) becomes

$$\begin{aligned} \mathcal{P}_\zeta = & \frac{H_\diamond^2}{\pi m_{\text{Pl}}^2 \epsilon_{1\diamond} c_{s\diamond}} (18e^{-3}) \left[1 - 2(D+1)\epsilon_{1\diamond} - D\epsilon_{2\diamond} \right. \\ & \left. + (D+2)\delta_{1\diamond} - (2\epsilon_{1\diamond} + \epsilon_{2\diamond} - \delta_{1\diamond}) \ln \frac{k}{k_\diamond} \right], \quad (53) \end{aligned}$$

where we have defined $D \equiv 1/3 - \ln 3$. From the above expression, one can already read off the spectral index of scalar perturbations,

$$n_s - 1 = -2\epsilon_{1\diamond} - \epsilon_{2\diamond} + \delta_{1\diamond}. \quad (54)$$

The standard expression is corrected by a term, $\delta_{1\diamond}$, which takes into account the time-dependence of the sound speed.

2. Tensor power spectrum

Although the equations of motion and evolution of the tensor perturbations are not affected by a varying sound speed in the scalar sector, there is however a subtle effect associated with the choice of the e-fold at which one evaluates the Hubble and sound flow functions entering the Taylor expansion of the power spectrum.

As shown in Ref. [43], around the pivot scale k_\diamond , the tensor power spectrum in the WKB, or uniform approximation, at first order in slow-roll, reads

$$\mathcal{P}_h(k) = \frac{16H_\diamond^2}{\pi m_{\text{Pl}}^2} (18e^{-3}) \left[1 - 2(D+1)\epsilon_{1\diamond} - 2\epsilon_{1\diamond} \ln \frac{k}{k_\diamond} \right], \quad (55)$$

where all background quantities are evaluated at the time η_\diamond such that

$$-k_\diamond \eta_\diamond = 1, \quad (56)$$

which is obviously different than η_\diamond in Eq. (52). It is therefore convenient to express H_\diamond and $\epsilon_{1\diamond}$ in terms of the parameters evaluated at $\eta = \eta_\diamond$. Using Eq. (48) with $\eta_\diamond = c_{s\diamond} \eta_\diamond$, at first order in the sound flow parameters, one gets

$$\begin{aligned} \mathcal{P}_h(k) = & \frac{16H_\diamond^2}{\pi m_{\text{Pl}}^2} (18e^{-3}) \left[1 - 2 \left(D + 1 + \ln \frac{1}{c_{s\diamond}} \right) \epsilon_{1\diamond} \right. \\ & \left. - 2\epsilon_{1\diamond} \ln \frac{k}{k_\diamond} \right]. \quad (57) \end{aligned}$$

Let us remark that, in the amplitude of the power spectrum, the coefficient in front of the first slow-roll parameter is different as compared to the standard case. Indeed, in the standard case, $c_{s\diamond} = 1$ and $\ln(1/c_{s\diamond})$ vanishes.

Eqs. (53) and (57) constitute one of the main result of this article. They represent the general scalar and tensor power spectra of k-inflation, valid at first order in the Hubble and sound flow parameters. In Ref. [45], they have recently been compared to the WMAP5 data [1, 2, 3, 4, 5, 6].

F. Running of the spectral index and higher order corrections

Having obtained the scalar perturbation power spectrum from the uniform approximation, we will now put this result to use in calculating the spectral index n_s and the running α_s of the spectral index using the method of Ref. [12]. Expanding the scalar perturbation power spectrum around the pivot scale k_\diamond in terms of $\ln(k/k_\diamond)$, one has

$$\mathcal{P}_\zeta(k) = \tilde{\mathcal{P}}_\zeta(k_\diamond) \sum_{n \geq 0} \frac{a_n}{n!} \ln^n \left(\frac{k}{k_\diamond} \right). \quad (58)$$

At zeroth order, the spectrum is given by the leading term of Eq. (53), namely

$$\tilde{\mathcal{P}}_\zeta(k_\diamond) = \frac{H_\diamond^2}{\pi m_{\text{Pl}}^2 \epsilon_{1\diamond} c_{s\diamond}} (18e^{-3}). \quad (59)$$

Since the physical power spectrum must not depend on the pivot scale, $d\mathcal{P}_\zeta(k)/d \ln k_\diamond = 0$, one may establish the recursion relation [12]

$$\begin{aligned} a_{n+1} = & \frac{d \ln \tilde{\mathcal{P}}_\zeta}{d \ln k_\diamond} a_n + \frac{da_n}{d \ln k_\diamond} \\ = & \frac{1}{1 - \epsilon_{1\diamond} + \delta_{1\diamond}} \left(\frac{da_n}{dN_\diamond} + \frac{d \ln \tilde{\mathcal{P}}_\zeta}{dN_\diamond} a_n \right), \quad n \geq 0, \quad (60) \end{aligned}$$

where in the last expression we have used

$$d \ln k_\diamond = (1 - \epsilon_{1\diamond} + \delta_{1\diamond}) dN_\diamond. \quad (61)$$

Using Eq. (59), one gets

$$\frac{d \ln \tilde{\mathcal{P}}_\zeta}{dN_\diamond} = -2\epsilon_{1\diamond} - \epsilon_{2\diamond} + \delta_{1\diamond}. \quad (62)$$

In terms of the expansion (58), the first coefficient a_0 is determined by the spectral amplitude, while a_1 is related to the spectral index, and a_2 to the running. Note that if we know a_0 to q th order in (ϵ_i, δ_i) , we can determine a_n to the order $q + n$. From the uniform approximation [see Eq. (53)] we know that

$$a_0 = 1 - 2(D+1)\epsilon_{1\diamond} - D\epsilon_{2\diamond} + (D+2)\delta_{1\diamond}, \quad (63)$$

at first order. The recurrence relation, up to second order, therefore gives

$$\begin{aligned} a_1 = & -2\epsilon_{1\diamond} - \epsilon_{2\diamond} + \delta_{1\diamond} + 2(2D+1)\epsilon_{1\diamond}^2 \\ & - (4D+3)\epsilon_{1\diamond}\delta_{1\diamond} + (2D-1)\epsilon_{1\diamond}\epsilon_{2\diamond} + D\epsilon_{2\diamond}^2 \\ & - D\epsilon_{2\diamond}\epsilon_{3\diamond} - (2D+1)\epsilon_{2\diamond}\delta_{1\diamond} + (D+1)\delta_{1\diamond}^2 \\ & + (D+2)\delta_{1\diamond}\delta_{2\diamond}. \end{aligned} \quad (64)$$

One more iteration of Eq. (60) allows to determine a_2 up to third order,

$$\begin{aligned} a_2 = & 4\epsilon_{1\diamond}^2 + 2\epsilon_{1\diamond}\epsilon_{2\diamond} - 4\epsilon_{1\diamond}\delta_{1\diamond} + \epsilon_{2\diamond}^2 - 2\epsilon_{2\diamond}\delta_{1\diamond} - \epsilon_{2\diamond}\epsilon_{3\diamond} \\ & + \delta_{1\diamond}^2 + \delta_{1\diamond}\delta_{2\diamond} + 6\epsilon_{1\diamond}^2\epsilon_{2\diamond} + 12D\epsilon_{1\diamond}^2\delta_{1\diamond} \\ & - (2D-1)\epsilon_{1\diamond}\epsilon_{2\diamond}^2 + 3(2D-1)\epsilon_{1\diamond}\epsilon_{2\diamond}\delta_{1\diamond} - 6D\epsilon_{1\diamond}\delta_{1\diamond}^2 \\ & + 3D\epsilon_{2\diamond}^2\delta_{1\diamond} - 3D\epsilon_{2\diamond}\delta_{1\diamond}^2 + D\delta_{1\diamond}^3 - 3D\epsilon_{2\diamond}\epsilon_{3\diamond}\delta_{1\diamond} \\ & + 3(D+1)\delta_{1\diamond}^2\delta_{2\diamond} - 8D\epsilon_{1\diamond}^3 + 2(2D-1)\epsilon_{1\diamond}\epsilon_{2\diamond}\epsilon_{3\diamond} \\ & - 6(D+1)\epsilon_{1\diamond}\delta_{1\diamond}\delta_{2\diamond} - D\epsilon_{2\diamond}^3 + 3D\epsilon_{2\diamond}^2\epsilon_{3\diamond} \\ & - 3(D+1)\epsilon_{2\diamond}\delta_{1\diamond}\delta_{2\diamond} - D\epsilon_{2\diamond}\epsilon_{3\diamond}^2 - D\epsilon_{2\diamond}\epsilon_{3\diamond}\epsilon_{4\diamond} \\ & + (D+2)\delta_{1\diamond}\delta_{2\diamond}^2 + (D+2)\delta_{1\diamond}\delta_{2\diamond}\delta_{3\diamond}. \end{aligned} \quad (65)$$

The relation between the a_i and n_s is obtained using the definition

$$n_s - 1 = \left(\frac{d \ln \mathcal{P}}{d \ln k} \right)_{k=k_\diamond}, \quad (66)$$

which, when compared to the corresponding derivative of Eq. (58), leads to

$$n_s - 1 = \frac{a_1}{a_0}, \quad (67)$$

and at second order in the Hubble and sound flow parameters, one gets

$$\begin{aligned} n_s - 1 = & -2\epsilon_{1\diamond} - \epsilon_{2\diamond} + \delta_{1\diamond} - 2\epsilon_{1\diamond}^2 - (2D+3)\epsilon_{1\diamond}\epsilon_{2\diamond} \\ & + 3\epsilon_{1\diamond}\delta_{1\diamond} + \epsilon_{2\diamond}\delta_{1\diamond} - D\epsilon_{2\diamond}\epsilon_{3\diamond} - \delta_{1\diamond}^2 \\ & + (D+2)\delta_{1\diamond}\delta_{2\diamond}. \end{aligned} \quad (68)$$

The same calculation can be repeated for the running. Its definition reads

$$\alpha_s = \left(\frac{d^2 \ln \mathcal{P}_\zeta}{d \ln^2 k} \right)_{k=k_\diamond}, \quad (69)$$

and it can be identified with

$$\alpha_s = \frac{a_2}{a_0} - \frac{a_1^2}{a_0^2}. \quad (70)$$

Up to second order, one finds

$$\alpha_s = -2\epsilon_{1\diamond}\epsilon_{2\diamond} - \epsilon_{2\diamond}\epsilon_{3\diamond} + \delta_{1\diamond}\delta_{2\diamond}, \quad (71)$$

We see that the parameter δ_2 appears in the above expression. Using the tools developed previously, one can even estimate the running at third order. The result reads

$$\begin{aligned} \alpha_s = & -2\epsilon_{1\diamond}\epsilon_{2\diamond} - \epsilon_{2\diamond}\epsilon_{3\diamond} + \delta_{1\diamond}\delta_{2\diamond} - 6\epsilon_{1\diamond}^2\epsilon_{2\diamond} + 5\epsilon_{1\diamond}\epsilon_{2\diamond}\delta_{1\diamond} \\ & + 4\epsilon_{1\diamond}\delta_{1\diamond}\delta_{2\diamond} - (2D+3)\epsilon_{1\diamond}\epsilon_{2\diamond}^2 - 2(D+2)\epsilon_{1\diamond}\epsilon_{2\diamond}\epsilon_{3\diamond} \\ & - D\epsilon_{2\diamond}\epsilon_{3\diamond}^2 - D\epsilon_{2\diamond}\epsilon_{3\diamond}\epsilon_{4\diamond} + 2\epsilon_{2\diamond}\epsilon_{3\diamond}\delta_{1\diamond} + \epsilon_{2\diamond}\delta_{1\diamond}\delta_{2\diamond} \\ & - 3\delta_{1\diamond}^2\delta_{2\diamond} + (D+2)\delta_{1\diamond}\delta_{2\diamond}^2 + (D+2)\delta_{1\diamond}\delta_{2\diamond}\delta_{3\diamond}. \end{aligned} \quad (72)$$

Finally, from the power spectrum of the tensor perturbations, the tensor to scalar ratio at first order in the Hubble and sound flow parameters reads

$$r = \frac{\mathcal{P}_h}{\mathcal{P}_\zeta} = 16c_{s\diamond}\epsilon_{1\diamond}. \quad (73)$$

We recover that since $c_s \leq 1$, r is reduced compared to the canonical single field dynamics.

We can compare our approach to the existing results in the literature, and, at first order, our results agree with those of Refs. [27, 28, 34, 35]. However, we would like to stress that at higher order, and in particular for the running, our results match only with those of Ref. [27]. Indeed, in Refs. [28, 34, 35], Eq. (24) is solved in terms of Bessel functions along the lines of the standard formalism which assumes that c_s is a constant. This ends up being an acceptable assumption at zeroth order only as is clear from Eq. (47). The spectral index at first order being, roughly speaking, the derivative of the power spectrum amplitude at zeroth order, one may indeed obtain its correct first order expression with the assumption that c_s is constant. However, if one wants to derive its quadratic corrections, or the running, then it is necessary to know the correct amplitude of the power spectra at first order. In Ref. [27], this goal was achieved using a conveniently chosen transformation of the time variable to absorb the time dependence of the sound speed, the resulting equation being integrable at first order.

This argument is at the heart of the present article. If the sound speed of the perturbations is a time-dependent quantity and if the first order expression (47) of c_s is inserted into Eq. (24), then the solution cannot be found by the usual technique. Therefore, the standard approach cannot be used and this prompts the use of a different method. This is what was done in Ref. [27], using a new time variable, and what is done in the present paper under the WKB/uniform approximation.

G. Model classification

To conclude this section, we generalize the classification of inflationary models of Ref. [12] to the DBI case. The energy density of a DBI inflaton field of Eq. (8) can be re-written as

$$\rho = \frac{\gamma^2}{\gamma + 1} \dot{\varphi}^2 + V(\varphi), \quad (74)$$

from which it is easy to see that we recover the standard expression in the limit $\gamma \rightarrow 1$. Let us refer to the first term in Eq. (74) as the kinetic energy contribution, while the second term represents the potential energy. The Hubble flow functions ϵ_1 and ϵ_2 then can be used to study the respective evolution of these contributions. With

$$\epsilon_1 = \frac{3\gamma\dot{\varphi}^2}{2\rho}, \quad (75)$$

$$\epsilon_2 = 2 \left(\frac{\ddot{\varphi}}{H\dot{\varphi}} + \epsilon_1 + \frac{1}{2}\delta_1 \right), \quad (76)$$

which represents the generalization of Eqs. (6) and (7) of Ref. [12], the change in the potential energy is given by

$$\dot{V} = -H\gamma\dot{\varphi}^2 \left[3 + \frac{\gamma}{\gamma + 1}(\epsilon_2 - 2\epsilon_1) + \frac{\gamma}{(\gamma + 1)^2}\delta_1 \right]. \quad (77)$$

Note that again the standard expressions are recovered for $\gamma \rightarrow 1$ since, in this case, also $\delta_1 \rightarrow 0$. From Eq. (77), we see that the potential energy density can never increase for small values of ϵ_i and δ_i even if γ is large.

The change for the ratio between kinetic and total energy density is given by

$$\frac{d}{dt} \left(\frac{\epsilon_1}{3} \right) = H \frac{\epsilon_1}{3} \epsilon_2. \quad (78)$$

Therefore, $\epsilon_2 = 0$ is the borderline between the regime where the kinetic energy contribution to ρ increases ($\epsilon_2 > 0$), and the regime where the kinetic energy contribution decreases ($\epsilon_2 < 0$). For a refined classification of DBI inflationary models, let us also calculate the time derivative of the kinetic energy density in Eq. (74):

$$\frac{d}{dt} \left(\frac{\gamma^2}{\gamma + 1} \dot{\varphi}^2 \right) = \frac{\gamma^2}{(\gamma + 1)^2} H \dot{\varphi}^2 [(\gamma + 1)(\epsilon_2 - 2\epsilon_1) + \delta_1]. \quad (79)$$

This equation can be viewed as the equivalent of Eq. (10) of Ref. [12]. Hence, the kinetic energy density increases while

$$\epsilon_2 > 2\epsilon_1 - \frac{\delta_1}{\gamma + 1}, \quad (80)$$

and decreases otherwise. We see that the standard condition, $\epsilon_2 - 2\epsilon_1 > 0$ or $\epsilon_2 - 2\epsilon_1 < 0$ is modified and that the sound flow parameter δ_1 now participates in the new criterion. This is natural since the factor γ appears in the expression of the kinetic energy. However, in the limit $\gamma \rightarrow +\infty$, the standard condition is also recovered.

III. EXAMPLE MODELS

We now illustrate our results in the case of DBI inflation with some specific choices of $V(\varphi)$ and $T(\varphi)$ considered in the literature. The DBI slow-roll trajectory permits to calculate the resulting values of γ and the first ϵ_i and δ_i parameters, and therefore the shape of the scalar primordial power spectrum through Eq. (53). As a warm up, we start with power-law inflation, where, as it is the case in the standard situation, exact solutions are available. Then we turn to the more important case of brane inflation that we discuss in some detail.

A. DBI power-law inflation

The DBI analogue of power-law inflation has been studied in Refs. [31, 32]. As we show in the following, it is particularly convenient for testing the previous approximations since the perturbation equations are exactly solvable in this case.

Looking for a power law behavior of the scale factor in terms of the conformal time, one finds that the warp function and the potential are given by [31, 32, 46]

$$T(\varphi) = T_0 \exp \left[-\sqrt{\frac{2\gamma\kappa}{p}}(\varphi - \varphi_0) \right], \quad (81)$$

$$V(\varphi) = V_0 \exp \left[-\sqrt{\frac{2\gamma\kappa}{p}}(\varphi - \varphi_0) \right], \quad (82)$$

where the two constants T_0 and V_0 are related by

$$V_0 = T_0 \frac{\gamma - 1}{\gamma} \left[\frac{3p}{2}(\gamma + 1) - \gamma \right]. \quad (83)$$

The solution of the Einstein equations are such that the Lorentz factor γ is a constant and the scale factor and scalar field can be expressed as

$$a(t) = a_0 \left(\frac{t}{t_0} \right)^p, \quad (84)$$

$$\varphi(t) = \varphi_0 + \sqrt{\frac{2p}{\kappa\gamma}} \ln \left(\frac{t}{t_0} \right). \quad (85)$$

In this case, one has also the relation

$$T_0 = \frac{2p\gamma}{\kappa t_0^2(\gamma^2 - 1)}. \quad (86)$$

In terms of conformal time η , the scale factor is also of the power-law form

$$a(\eta) = \ell_0 |\eta|^{1+\beta}, \quad (87)$$

with

$$\beta = -\frac{2p - 1}{p - 1}. \quad (88)$$

One can check that when $p \rightarrow \infty$, β goes to -2 and one recovers the de Sitter case.

Let us now turn to the calculation of the perturbations. The equation of motion (24) for the Mukhanov-Sasaki variable takes the form

$$v_{\mathbf{k}}'' + \left[\frac{k^2}{\gamma^2} - \frac{\beta(\beta+1)}{\eta^2} \right] v_{\mathbf{k}} = 0, \quad (89)$$

where γ is now a constant. This equation can be solved explicitly in terms of Bessel functions and the solution reads

$$v_{\mathbf{k}}(\eta) = (k\eta)^{1/2} \left[A_{\mathbf{k}} J_{\beta+1/2} \left(\frac{k\eta}{\gamma} \right) + B_{\mathbf{k}} J_{-(\beta+1/2)} \left(\frac{k\eta}{\gamma} \right) \right], \quad (90)$$

where $A_{\mathbf{k}}$ and $B_{\mathbf{k}}$ are two scale-dependent arbitrary constants. As usual, one requires the initial state, evaluated in the limit $k\eta/\gamma \rightarrow -\infty$ to be of the WKB type. This completely fixes $A_{\mathbf{k}}$ and $B_{\mathbf{k}}$ which are given by

$$A_{\mathbf{k}} = -B_{\mathbf{k}} e^{i\pi(\beta+1/2)}, \quad (91)$$

$$B_{\mathbf{k}} = \sqrt{\frac{\pi}{4k}} \frac{e^{i\pi(\beta+1/2)/2 - i\pi/4}}{\cos(\pi\beta)}. \quad (92)$$

The function (90) is now completely specified. Using the asymptotic behavior of the Bessel functions in the limit $k\eta/\gamma \rightarrow 0$, one obtains the power spectrum from Eq. (27)

$$\mathcal{P}_{\zeta} = \frac{\gamma h(\beta)}{\pi m_{\text{Pl}}^2 \ell_0^2 \epsilon_1} \left(\frac{k}{\gamma} \right)^{2\beta+4}, \quad (93)$$

where the function $h(\beta)$ stands for

$$h(\beta) = \frac{\pi}{2^{2\beta+2} \cos^2(\pi\beta) \Gamma^2(\beta+3/2)}. \quad (94)$$

In the above expression, Γ is the Euler function of first kind. In the de Sitter case, $h(-2) = 1$. Let us also notice that, in the case of power-law inflation, the first slow-roll parameter ϵ_1 is actually constant and given by

$$\epsilon_1 = \frac{2+\beta}{1+\beta}. \quad (95)$$

As usual, for $\beta = -2$, one recovers $\epsilon_1 = 0$.

We can now compare the previous expression with the one obtained in the uniform approximation. The integral (40) reads

$$\frac{2}{3} f^{3/2}(k, \eta) = \int_{\eta_*}^{\eta} d\tau \sqrt{\frac{(\beta+1/2)^2}{\tau^2} - \frac{k^2}{\gamma^2}}, \quad (96)$$

where, as already mentioned above, γ is, in the present context, a constant. This integral can be performed exactly. Then, straightforward calculations lead to

$$\mathcal{P}_{\zeta} = \frac{\gamma j(\beta)}{\pi m_{\text{Pl}}^2 \ell_0^2 \epsilon_1} \left(\frac{k}{\gamma} \right)^{2\beta+4}, \quad (97)$$

where the function $j(\beta)$ can be expressed as

$$j(\beta) = \frac{2e^{2\beta+1}}{(2\beta+1)^{2\beta+2}}. \quad (98)$$

The above power spectrum is the analogue of Eq. (58) in Ref. [43]. In particular, the function $j(\beta)$ is exactly the same as in the standard case. Therefore the error in the amplitude of the power spectrum in the WKB/uniform approximation is similar (see Fig. 1 of Ref. [43]). In particular, and as already mentioned, it is around 10% for $\beta \sim -2$, i.e. close to scale invariance. For $\beta < -2$, when the spectrum is not necessarily close to the Harrison-Zeldovitch spectrum, the accuracy of the WKB/uniform approximation becomes better. Let us also mention that Ref. [44] has discussed how to improve the precision on the amplitude and the method developed in that article may be applied here. As can be noticed on the above equations, it turns out that the spectral index is predicted exactly in the case of (DBI) power-law inflation.

B. Brane Inflation

We now apply our formalism to the case of the brane inflationary models discussed in Refs. [42, 47, 48, 49, 50]. In these scenarios, the warp function and potential are given by the following expressions

$$T(\varphi) = \frac{\varphi^4}{\lambda}, \quad V(\varphi) = \frac{V_0}{1 + \left(\frac{\mu}{\varphi} \right)^4} + \frac{\varepsilon}{2} m^2 \varphi^2. \quad (99)$$

Here, the factor ε stands for $\varepsilon = \pm 1$ and the positive sign corresponds to the so-called ‘‘Ultra-Violet’’ (UV) models while the minus sign refers to the ‘‘Infra-Red’’ (IR) scenarios [42]. The Coulomb potential is due to the attraction between a $\bar{D}3$ -brane sitting at the bottom of the throat and a mobile $D3$ -brane, for a review see Ref. [40]. The quadratic correction in Eq. (99) has a different status. It is a phenomenological description of the brane moduli potential and its shape is not established as neatly as for the Coulomb potential. The above described model is characterized by four parameters, the mass m , the scale μ , the dimensionless ‘t Hooft constant λ and V_0 (whose dimension is m_{Pl}^4). In the following it will become clear that the evolution of the field is in fact controlled by two dimensionless parameters α and β . The parameter α is defined by

$$\alpha \equiv \frac{12\pi m_{\text{Pl}}^2}{\lambda m^2} = \frac{96\pi^2}{\kappa \lambda m^2}, \quad (100)$$

while the other dimensionless parameter β is given by

$$\beta \equiv \frac{V_0}{m^2 m_{\text{Pl}}^2}. \quad (101)$$

Physically, β measures the importance of the constant term relative to the mass term in the potential.

For those models, the vacuum expectation value (vev) of the inflaton field possesses a geometrical interpretation, namely the distance between the two branes living in the throat. As a consequence, it can be written as $\varphi = \sqrt{T_3}r$, where $T_3 = 1/[(2\pi)^3 g_s \alpha'^2]$ is the tension of the brane, g_s being the string coupling, α' the string scale and r the radial coordinate along the throat. Notice that we do not consider a possible angular motion of the brane [51, 52]. In order for the moving brane to be inside the throat, one should impose $r < r_{\text{uv}}$ where r_{uv} is the coordinate at which the throat is connected to the bulk. This quantity can be written as [53]

$$r_{\text{uv}}^4 = 4\pi g_s \alpha'^2 \frac{\mathcal{N}}{v}, \quad (102)$$

where \mathcal{N} is a positive integer representing the total Ramond–Ramond (RR) charge and v represents the dimensionless ratio of the five-dimensional volume forming the basis of the six-dimensional conifold geometry to the volume of the unit five-sphere. Requiring the volume of the throat to be smaller than the total volume of the extra-dimensions amounts to

$$\varphi < \varphi_{\text{uv}} < \frac{m_{\text{Pl}}}{\sqrt{2\pi\mathcal{N}}}, \quad (103)$$

and inflation always occurs for sub-Planckian values of φ . On the other hand, the bottom of the throat is located at r_0 and, hence, one must have $\varphi > \varphi_0 \equiv \sqrt{T_3}r_0$. Moreover, for the model to be valid, the (physical) distance between the brane must be larger than the string length and one can show that this amounts to

$$\varphi > \varphi_{\text{strg}} \equiv \varphi_0 e^{\sqrt{\alpha'} r_{\text{uv}}}. \quad (104)$$

Notice also that the parameters of the potential (99) can be calculated in terms of the stringy parameters. The tension $T(\varphi)$, in the model under consideration, can also be written as $T(\varphi) = T_3(\varphi/\varphi_{\text{uv}})^4$ which implies that [42]

$$\lambda = \frac{\mathcal{N}}{2\pi^2 v}. \quad (105)$$

The constant term V_0 is given by $V_0 = 4\pi^2 v \varphi_0^4 / \mathcal{N}$ which can also be expressed as

$$V_0 = 2h^4(r_0)T_3, \quad (106)$$

where $h(\varphi) \equiv \varphi/\varphi_{\text{uv}}$ is the warp factor. On the other hand, the constant μ can be expressed as $\mu^4 = \varphi_0^4 / \mathcal{N}$.

Finally, from the requirement that the volume of the throat is smaller than the total volume of the extra-dimensions, one deduces that [42]

$$\sqrt{\frac{\beta}{\alpha}} < \frac{1}{\sqrt{24\pi^3}} \frac{h^2(r_0)}{\mathcal{N}} \ll 1. \quad (107)$$

We now study the different types of inflation that can occur in the scenario under consideration. Each type corresponds to a different choice of the parameters characterizing the model as discussed in Ref. [42] where the overall situation is summarized on two phase diagrams.

1. KKLM MT model

The quadratic term in Eq. (99) can be neglected in the case where $V_0/m^2 \gg m_{\text{Pl}}^2 > \varphi^2$ or, in other words, for $\beta \gg 1$. This, in turn, implies that $\alpha \gg 1$ because of Eq. (107). This limit corresponds to the KKLM MT model [19, 40]. The trajectory given by Eq. (20) reads

$$N(\varphi) = -\kappa \int^\varphi d\psi \sqrt{\frac{2}{3\kappa} + \frac{\mu^2}{16} \left(\frac{\psi}{\mu}\right)^{10} \left[1 + \left(\frac{\mu}{\psi}\right)^4\right]}. \quad (108)$$

The field rolls down the potential (i.e. φ is decreasing) while inflation is under way and we always have $\varphi > \mu$. Therefore, the previous expression can be approximated by

$$N(\varphi) \simeq -\frac{\kappa\mu^2}{4} \left[\frac{1}{6} \left(\frac{\varphi}{\mu}\right)^6 + \frac{1}{2} \left(\frac{\varphi}{\mu}\right)^2 - \frac{1}{4} \left(\frac{\mu}{\varphi}\right)^2 - \frac{4}{3\kappa\mu^2} \left(\frac{\mu}{\varphi}\right)^4 \right]_{\varphi_{\text{ini}}}^{\varphi}. \quad (109)$$

For $\varphi \gg \mu$, the first two terms in this expression clearly dominate. In fact, this is precisely the trajectory found in Ref. [40] in the limit where the DBI dynamics can be ignored. Therefore, the last two terms can be understood as the DBI corrective terms induced by the non-standard kinetics. Clearly, these corrections do not play an important role in the case of KKLM MT as long as $\epsilon_1 \ll 1$. As shown in Ref. [40], the DBI effects can only be significant for $\epsilon_1 > 1$ and we therefore do not proceed further with the KKLM MT model¹.

2. Chaotic Klebanov–Strassler models

We now move on to the model where the quadratic correction dominates (hence $\varepsilon = +1$) the potential. This corresponds to the condition $\beta \ll 1$ and to the scenario considered in Refs. [20, 39], which we refer to as chaotic Klebanov–Strassler (CKS) inflation. The potential and warp function in this case read

$$V(\varphi) = \frac{1}{2} m^2 \varphi^2, \quad T(\varphi) = \frac{\varphi^4}{\lambda}. \quad (110)$$

The two remaining parameters are the mass m and the dimensionless constant λ . The integration of Eq. (20)

¹ It was also shown in that reference that, depending on the values of the string parameters α' and g_s (i.e. the string coupling), the end of inflation can occur either by violation of the slow-roll conditions or by instability. In the first case, the spectral index is given by $n_s \simeq 0.97$ while it is $n_s \simeq 1$ in the other situation.

can be performed explicitly and gives

$$\frac{\alpha^{1/2}}{2\pi}N = -\sqrt{1+x^4} + \sqrt{1+x_{\text{ini}}^4} - 2\ln \frac{x}{x_{\text{ini}}} + \ln \left(\frac{1+\sqrt{1+x^4}}{1+\sqrt{1+x_{\text{ini}}^4}} \right), \quad (111)$$

where we have defined

$$x^4 \equiv \alpha(\varphi/m_{\text{Pl}})^4. \quad (112)$$

This is the implicit slow roll trajectory; in general, inverting this expression to find $\varphi(N)$ is analytically impossible. However, φ decreases during inflation, therefore the initial field value φ_{ini} is necessarily larger than all the field values φ attained during inflation. Assuming $\varphi \ll \varphi_{\text{ini}}$, an approximate inversion gives

$$\varphi \simeq \varphi_{\text{ini}} \exp \left(-\alpha^{1/2} \frac{N}{4\pi} \right). \quad (113)$$

This expression is nothing but the solution $\varphi \rightarrow 1/t$ found in Ref. [39] but expressed in terms of the number of e-folds.

We can also derive the behavior of γ , ϵ_i and δ_i . Using Eq. (17) together with Eq. (18) in the limit where $\epsilon_1 \ll 1$, we find the following expression for the Lorentz factor:

$$\gamma(\varphi) \simeq \left(\frac{m_{\text{Pl}}}{\varphi} \right)^2 \sqrt{\frac{\varphi^4}{m_{\text{Pl}}^4} + \frac{1}{\alpha}}. \quad (114)$$

Note that $\gamma \rightarrow \infty$ as $\varphi \rightarrow 0$, i.e. the ultra-relativistic limit is attained at late times. Likewise, with the help of Eq. (18), we find for ϵ_1

$$\epsilon_1 \simeq \frac{1}{4\pi} \left(\frac{\varphi^4}{m_{\text{Pl}}^4} + \frac{1}{\alpha} \right)^{-1/2}. \quad (115)$$

Note that ϵ_1 approaches a constant as $\varphi \rightarrow 0$

$$\lim_{\varphi \rightarrow 0} \epsilon_1 = \frac{\sqrt{\alpha}}{4\pi}. \quad (116)$$

We recover that, in order to have slow-roll inflation for small values of φ , the parameters of the model, m and λ , must be such that $\alpha \ll 1$.

The above expression has also an important consequence with respect to the end of inflation in this model. Indeed, the condition $\epsilon_1 = 1$ reduces to

$$\frac{\varphi_{\text{end}}}{m_{\text{Pl}}} = \left(\frac{1}{16\pi^2} - \frac{1}{\alpha} \right)^{1/4}. \quad (117)$$

Since we are in the limit $\alpha \ll 1$, this means that inflation cannot stop by violation of the slow-roll conditions. It must be stopped by another mechanism, typically by instability, comparable to the case of standard hybrid inflation. The end of inflation φ_{end} hence becomes a free,

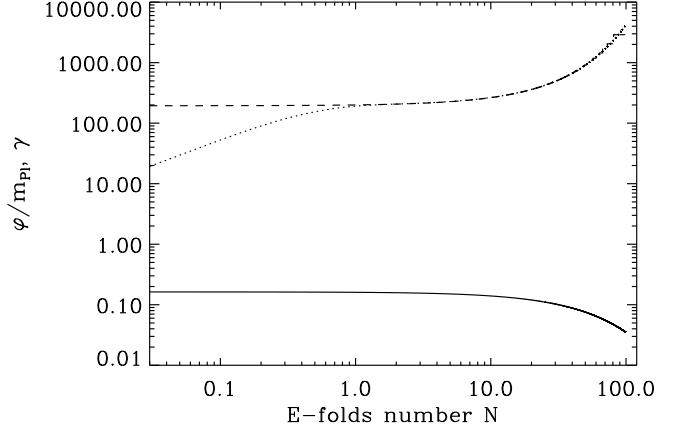


FIG. 2: Evolution of the scalar field φ (solid line) and of the Lorentz factor γ (dotted and dashed lines) as a function of the number of e-folds N , for $\alpha \simeq 0.04$ ($m = 0.01m_{\text{Pl}}$, $\lambda = 10^7$). The initial value of the inflaton field is such that $\gamma_{\text{ini}} = 3$. The solid line represents the trajectory of the inflaton field computed from the exact equation of motion. The DBI slow-roll trajectory of Eq. (111) cannot be distinguished from the exact one on this plot. Concerning γ , except during a short transient regime at the beginning of inflation, the two curves also match.

additional parameter of the model, which is notably crucial for normalizing predictions to CMB observations [54].

The accuracy of the DBI slow-roll trajectory can be assessed by an exact numerical integration of the equations of motion. The results are plotted in Fig. 2 and confirm that, except during a few e-folds after the beginning of inflation, the DBI slow-roll approximation is accurate. Similarly, the other Hubble flow functions can be approximated by

$$\epsilon_2 \simeq \frac{1}{2\pi} \left(\frac{\varphi}{m_{\text{Pl}}} \right)^4 \left(\frac{\varphi^4}{m_{\text{Pl}}^4} + \frac{1}{\alpha} \right)^{-3/2}, \quad (118)$$

$$\epsilon_3 \simeq -\frac{1}{\pi} \left(-\frac{1}{2} \frac{\varphi^4}{m_{\text{Pl}}^4} + \frac{1}{\alpha} \right) \left(\frac{\varphi^4}{m_{\text{Pl}}^4} + \frac{1}{\alpha} \right)^{-3/2}, \quad (119)$$

where Eq. (19) has been used. As a result,

$$\lim_{\varphi \rightarrow 0} \epsilon_2 = 0, \quad \lim_{\varphi \rightarrow 0} \epsilon_3 = -\frac{\sqrt{\alpha}}{\pi} \sim -4\epsilon_1. \quad (120)$$

Concerning the sound flow functions, one gets

$$\delta_1 \simeq \frac{1}{2\pi\alpha} \left(\frac{\varphi^4}{m_{\text{Pl}}^4} + \frac{1}{\alpha} \right)^{-3/2}, \quad (121)$$

$$\delta_2 \simeq \frac{3}{2\pi} \left(\frac{\varphi}{m_{\text{Pl}}} \right)^4 \left(\frac{\varphi^4}{m_{\text{Pl}}^4} + \frac{1}{\alpha} \right)^{-3/2}. \quad (122)$$

Similarly, for small values of φ

$$\lim_{\varphi \rightarrow 0} \delta_1 = \frac{\sqrt{\alpha}}{2\pi} \sim 2\epsilon_1, \quad \lim_{\varphi \rightarrow 0} \delta_2 = 0. \quad (123)$$

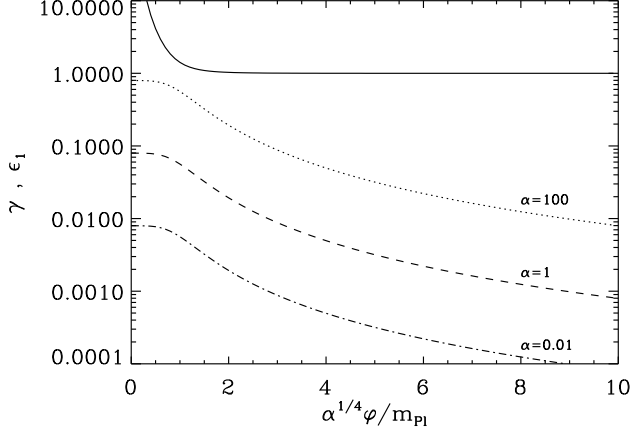


FIG. 3: Exact numerical evolution of the Lorentz factor γ (solid line) and ϵ_1 as a function of the renormalized field value $\alpha^{1/4}\varphi/m_{\text{Pl}}$ and for various values of the parameter α . Notice that inflation proceeds from larger towards smaller field values. As can be seen from Eq. (114), the α -dependence of the Lorentz factor γ is in the renormalized field. One can check that the asymptotic values of ϵ_1 are compatible with the slow-roll predictions given in Eq. (115) (see also Fig. 4).

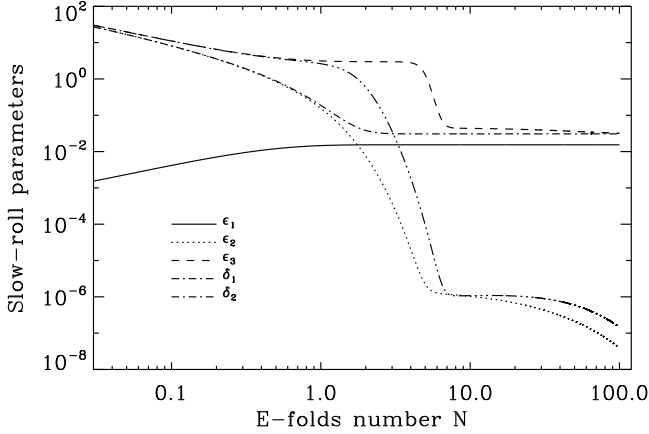


FIG. 4: Exact numerical evolution of the slow-roll parameters as a function of the number of e-folds N . The other parameters are the same as in Fig. 3.

The evolution of the DBI slow-roll parameters is represented in Fig. 3 and Fig. 4 and compared to an exact numerical integration of the equations of motion. Again, apart during the few e-folds of the transient regime, the DBI slow-roll trajectory and parameters are in good agreement with the exact integration.

As already noticed before and as clearly shown in Figs. 2 and 3, the Lorentz factor γ goes to infinity while $\varphi \rightarrow 0$. In this case, one may question the use of the

inflationary flow formalism (besides the fact that it is hard to interpret since there is no natural measure in parameter space) where the Hubble scale $H(\varphi)$ and $\gamma(\varphi)$ are expanded in terms of the inflaton field at a specific order [28].

Owing to the above analytical expressions, we can now easily consider the observational predictions of this scenario. The multipole moments at large angular scales are given by

$$C_\ell \simeq \frac{2H^2\gamma}{25m_{\text{Pl}}^2\epsilon_1} \frac{1}{\ell(\ell+1)}, \quad (124)$$

which, for $\ell = 2$, gives the quadrupole moment

$$\frac{Q}{T_{\text{cmb}}} = \sqrt{\frac{5C_2}{4\pi}} \simeq 6 \times 10^{-6}. \quad (125)$$

The various quantities appearing in the above expressions should be evaluated at “sound horizon crossing”. Using the trajectory (113)

$$\varphi_* = \varphi_{\text{end}} e^{\sqrt{\alpha}N_*/(4\pi)}, \quad (126)$$

where N_* is the number of e-folds between the end of inflation and the sound horizon crossing. It is usually considered that $40 < N_* < 60$. However, for the model under consideration, we have $\gamma \propto 1/\varphi^2$ and $H^2 \propto \varphi^2$ and, therefore, these two terms cancel out of Eq. (124). Since $\epsilon_1 \sim \sqrt{\alpha}/(4\pi)$, we have in fact the remarkable property that the multipole moments do not depend on the number of e-folds between sound horizon crossing and the end of inflation. This property was first noticed in Ref. [50]. Working out the previous expressions, one arrives at

$$\frac{1}{\alpha} \left(\frac{m}{m_{\text{Pl}}} \right)^2 = \frac{45}{4\pi} \frac{Q^2}{T_{\text{cmb}}^2} \simeq 1.3 \times 10^{-10}. \quad (127)$$

Since $\alpha \ll 1$, this means that the mass m should be smaller than in the standard chaotic scenario. The previous expression can be re-expressed in terms of the parameter λ ,

$$\lambda \left(\frac{m}{m_{\text{Pl}}} \right)^4 = 125 \frac{Q^2}{T_{\text{cmb}}^2} \simeq 0.0083. \quad (128)$$

Inserting Eqs. (120) and (123) into the expression of the scalar spectral index derived in Sec. II E 1, one obtains

$$n_s - 1 = \mathcal{O}(\epsilon^3, \delta^3, \epsilon^i \delta^j), \quad i + j = 3. \quad (129)$$

The spectral index vanishes at first order in agreement with the results of Refs. [20, 27]. Here, we find that, for this model, this also the case at second order. Notice also that from Eq. (100), the second and third-order contribution in the running of the spectral index vanishes for $\varphi \rightarrow 0$ and α_s reads

$$\alpha_s = \mathcal{O}(\epsilon^4, \delta^4, \epsilon^i \delta^j), \quad i + j = 4. \quad (130)$$

Let us notice however that, although extremely small, the actual value of α_s obtained from the DBI slow-roll approximation is significantly different than the value obtained from the numerical integration, typically at almost 100%. Such a loss of accuracy is related to the extremely flat power spectrum which has an almost vanishing running; as for de Sitter, such a limit is in fact singular for the scalar modes. In any case, such a running is by far too small to be detectable in any of the present and planned cosmological experiments.

Then, one can compare the above predictions with the WMAP5 [1, 2, 3, 4, 5, 6] constraints on the CMB power spectra established in Ref. [45]. Notice that, in order to perform this comparison, it is mandatory to use a theoretical power spectrum which takes into account the fact that the sound speed is a time-dependent quantity. It would be inconsistent to do this comparison using the constraints on the ordinary slow-roll parameters established, for instance, in Refs. [54, 55]. From Ref. [45], we see that, in absence of a significant contribution of gravitational waves, a red tilt is favored. Therefore, the present model which is scale-invariant to a very high accuracy is clearly disfavored by the current data.

Let us remind that the model is also strongly disfavored by the WMAP non-gaussianity bounds, as shown in Ref. [20]. Indeed, at leading order for DBI models, the parameter f_{NL} is given by [26, 56]

$$f_{\text{NL}} = \frac{35}{108} (1 - \gamma^2) \simeq -\frac{35}{108} \gamma^2 \quad (131)$$

which, in the present context, gives

$$f_{\text{NL}} \simeq -\frac{35}{108\alpha} \left(\frac{m_{\text{Pl}}}{\varphi} \right)^4. \quad (132)$$

The constraint $\varphi < \varphi_{\text{UV}}$ implies [42]

$$f_{\text{NL}} > -\frac{35\pi^2}{27} \frac{\mathcal{N}^2}{\alpha} \gg 1, \quad (133)$$

because $\mathcal{N} > 1$ and $\alpha \ll 1$. The above inequality is in contradiction with the observational range $-151 \leq f_{\text{NL}} \leq 253$ (see Ref. [6]).

3. Chaotic Klebanov Strassler models with constant term

We now consider the case where the Coulomb term is negligible and the potential can be written as

$$V(\varphi) = V_0 + \frac{\varepsilon}{2} m^2 \varphi^2, \quad (134)$$

while the warp function remains unchanged and given by its expression in Eq. (99). These models have been discussed in Refs. [42, 47, 48, 49, 50].

Using Eqs. (16) and (19) leads to $\dot{\varphi} = -\varepsilon m^2 \varphi / (3\gamma H)$. This means that, in the UV ($\varepsilon = 1$) case, the vev of the inflaton field is decreasing as inflation proceeds while

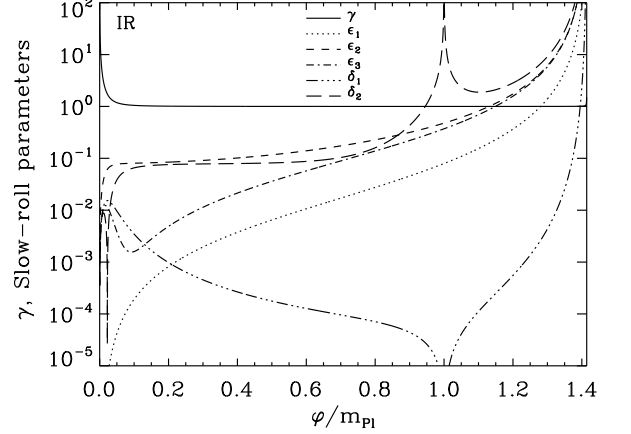


FIG. 5: Evolution of the Lorentz factor γ and of the Hubble and sound flow functions in the IR case of the CKS models with constant term. The parameters are $\alpha = 500$ and $\beta = 1$. Inflation proceeds from left to right and the “divergence” occurs at $\varphi/m_{\text{Pl}} \rightarrow \sqrt{2\beta}$.

it is increasing in the IR case ($\varepsilon = -1$). In order to understand in which regimes DBI inflation can occur, it is convenient to express the Lorentz factor in terms of the vacuum expectation value of the inflaton field as

$$\gamma(\varphi) = \left(\frac{m_{\text{Pl}}}{\varphi} \right)^2 \left[\left(\frac{\varphi}{m_{\text{Pl}}} \right)^4 + \frac{1}{\alpha} \frac{(\varphi/m_{\text{Pl}})^2}{2\beta + \varepsilon (\varphi/m_{\text{Pl}})^2} \right]^{1/2}. \quad (135)$$

Of course, when $\varepsilon = +1$ and $\beta = 0$, one checks that Eq. (114) is recovered. The DBI regime, $\gamma \rightarrow +\infty$, is obtained when $\varphi \rightarrow 0$. In this case, γ can be approximately written as

$$\gamma \simeq \frac{1}{\sqrt{2\alpha\beta}} \frac{m_{\text{Pl}}}{\varphi}. \quad (136)$$

Let us notice that this last equation is valid for $\varepsilon = \pm 1$. In addition, in the IR case, the Lorentz factor also blows up when $\varphi \rightarrow m_{\text{Pl}} \sqrt{2\beta}$ as

$$\gamma_{\text{IR}} \simeq \frac{1}{\sqrt{2\alpha\beta}} \left[2\beta - \left(\frac{\varphi}{m_{\text{Pl}}} \right)^2 \right]^{-1/2}. \quad (137)$$

The evolution of $\gamma(\varphi)$ is displayed in Figs. 5 and 6. Notice that we must always have $\varphi < m_{\text{Pl}} \sqrt{2\beta}$ in order to guarantee the positivity of the potential. Moreover, since in the limit $\varphi \rightarrow m_{\text{Pl}} \sqrt{2\beta}$, $V(\varphi) \rightarrow 0$, the corrections to the potential may become non-negligible. In particular, the Coulomb part of the potential that we have neglected in this subsection will become important again. Notice that this situation is rather similar to the case of small field models in standard inflation where the potential is given by $V \propto 1 - \phi^2$ and where, at the end of the slow-roll phase, it is necessary to add higher order terms of

the form ϕ^p in order for the potential to have a minimum which ensures that the reheating can proceed. We conclude that the limit $\varphi \rightarrow m_{\text{Pl}}\sqrt{2\beta}$, although it does imply $\gamma \rightarrow +\infty$, appears to be more difficult to realize from the physical point of view.

For all ε , the first slow-roll parameter can be written as

$$\epsilon_1(\varphi) = \frac{1}{4\pi\gamma(\varphi)} \frac{(\varphi/m_{\text{Pl}})^2}{\left[2\beta + \varepsilon(\varphi/m_{\text{Pl}})^2\right]^2}, \quad (138)$$

which, in the limit $\varphi \rightarrow 0$, becomes

$$\epsilon_1 \simeq \frac{1}{16\pi} \sqrt{\frac{2\alpha}{\beta^3}} \left(\frac{\varphi}{m_{\text{Pl}}}\right)^3, \quad (139)$$

and goes to zero as the inflaton vev vanishes. This means that, in the UV case, where the field decreases from some initial value towards zero, inflation cannot stop by violation of the slow-roll condition.

On the contrary, in the IR case, the field starts from a value close to zero and increases. As already mentioned, the vev of the field is bounded by $\sqrt{2\beta}$. In this limit, the first slow-roll parameter blows up as

$$\epsilon_1 \simeq \frac{\sqrt{8\alpha\beta^3}}{4\pi} \left[2\beta - \left(\frac{\varphi}{m_{\text{Pl}}}\right)^2\right]^{-3/2}, \quad (140)$$

and contrary to the UV case, inflation will stop by violation of the slow-roll conditions. The evolution of ϵ_1 is displayed in Fig. 5 (IR case) and in Fig. 6 (UV case).

It is also interesting to establish the expression of the other slow-roll parameters. Lengthy but straightforward calculations lead to the following expressions

$$\epsilon_2 = 4\epsilon_1 - \delta_1 - \frac{\varepsilon\alpha}{2\pi} \frac{\varphi^2}{m_{\text{Pl}}^2} \frac{\gamma^2 - 1}{\gamma}, \quad (141)$$

$$\begin{aligned} \epsilon_3 &= 4\epsilon_1 - \frac{\delta_1\delta_2}{\epsilon_2} + \frac{\alpha^2}{4\pi^2\epsilon_2} \frac{\varphi^4}{m_{\text{Pl}}^4} \frac{(\gamma^2 - 1)^2}{\gamma^2} \\ &\quad - \frac{\varepsilon\alpha}{2\pi} \frac{\delta_1}{\epsilon_2} \frac{\varphi^2}{m_{\text{Pl}}^2} \frac{\gamma^2 + 1}{\gamma}, \end{aligned} \quad (142)$$

$$\delta_1 = \frac{\varepsilon\epsilon_1}{\alpha\gamma^2} \frac{m_{\text{Pl}}^4}{\varphi^4} \left[1 + \varepsilon\alpha \frac{\varphi^4}{m_{\text{Pl}}^4} (\gamma^2 - 1)\right], \quad (143)$$

$$\begin{aligned} \delta_2 &= \epsilon_2 - 2\delta_1 + \frac{\varepsilon\alpha}{\pi\gamma} (\gamma^2 - 1) \frac{\varphi^2}{m_{\text{Pl}}^2} \\ &\quad + \varepsilon\alpha\gamma^2 \frac{\varphi^4}{m_{\text{Pl}}^4} \left[1 + \varepsilon\alpha (\gamma^2 - 1) \frac{\varphi^4}{m_{\text{Pl}}^4}\right]^{-1} \\ &\quad \times \left[2\delta_1 - \frac{\varepsilon\alpha}{\pi\gamma} \frac{(\gamma^2 - 1)^2}{\gamma^2} \frac{\varphi^2}{m_{\text{Pl}}^2}\right]. \end{aligned} \quad (144)$$

These functions are represented in Fig. 5 for the IR case ($\varepsilon = -1$) and in Fig. 6 in the UV case ($\varepsilon = +1$).

With a constant term included, Eq. (20) describing the field trajectory becomes significantly more complicated.

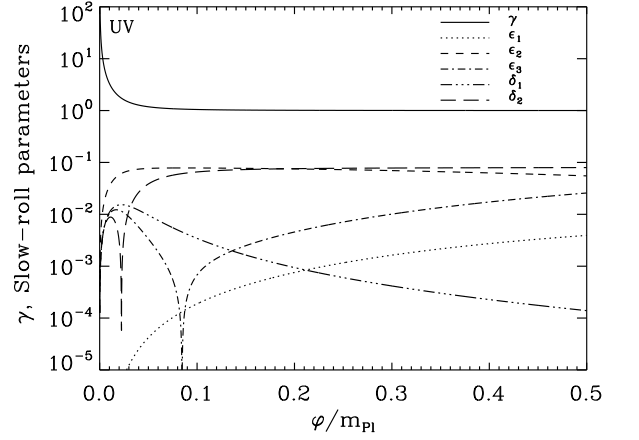


FIG. 6: Same as Fig. 5 but in the UV case. The inflaton field decreases while inflation is under way.

Expressed in terms of the parameters α and β , the DBI trajectory reads

$$\begin{aligned} N(\varphi) &= -2\pi\varepsilon\beta \int_{u_{\text{ini}}}^u du (u - \varepsilon)^{-3/2} \\ &\quad \times \left[u^3 + \varepsilon u^2 + \left(\frac{\varepsilon}{\alpha\beta^2} - 1\right)u + \frac{1}{\alpha\beta^2} - \varepsilon\right]^{1/2}, \end{aligned} \quad (145)$$

where we have defined the new dimensionless variable u by

$$u \equiv \frac{1}{\beta} \left(\frac{\varphi}{m_{\text{Pl}}}\right)^2 + \varepsilon. \quad (146)$$

The expression (145) is an elliptic integral and can be expressed in terms of the canonical elliptic integrals of the first and second kind, respectively denoted as in Ref. [57] by $F(\theta|p)$ and $E(\theta|p)$. We will further use the definition

$$n \equiv \frac{\alpha\beta^2}{\alpha\beta^2 - \varepsilon}. \quad (147)$$

To ensure that all expressions are well-defined in the following, we now consider separately the case of IR and UV models.

For the IR case, $\varepsilon = -1$ and it follows from Eq. (146) that the variable u maps the range $\varphi/m_{\text{Pl}} \in [0, \sqrt{2\beta}]$ to $u \in [-1, 1]$. From Eq. (147), we see that $0 < n < 1$ and both u and n appearing in Eq. (145) are in the canonical domain of definition of the elliptic integrals $E(\theta|p)$ and $F(\theta|p)$ (see Ref. [57]). One gets

$$N_{\text{IR}}(\varphi) = 2\pi\beta \left[\frac{2}{\sqrt{n}} F(\arcsin u | n) - \frac{2}{\sqrt{n}} F(\arcsin u_{\text{ini}} | n) - \frac{3}{\sqrt{n}} E(\arcsin u | n) + \frac{3}{\sqrt{n}} E(\arcsin u_{\text{ini}} | n) \right. \\ \left. - 2 \ln \left(\frac{\sqrt{1 - u_{\text{ini}}^2} + \sqrt{1/n - u_{\text{ini}}^2}}{\sqrt{1 - u^2} + \sqrt{1/n - u^2}} \right) - 2(1 - u) \sqrt{\frac{1/n - u^2}{1 - u^2}} + 2(1 - u_{\text{ini}}) \sqrt{\frac{1/n - u_{\text{ini}}^2}{1 - u_{\text{ini}}^2}} \right]. \quad (148)$$

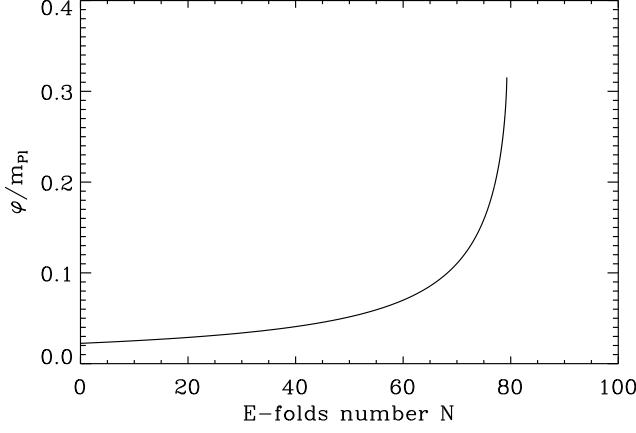


FIG. 7: Typical evolution of the scalar field φ according to Eq. (148) in the IR case. The parameters are $\alpha = 4$ and $\beta = 0.05$ such that the condition $\beta/\alpha \ll 1$ is satisfied. The initial condition is $\varphi_{\text{ini}}/m_{\text{Pl}} \simeq 0.022$ and one can check that the field value always remains sub-Planckian. With the parameters considered here, one has $n = 0.1$, i.e. $0 < n < 1$ as required for the IR case.

A typical IR trajectory is represented in Fig. 7. This expression, although exact, is quite involved. Therefore, it is interesting to consider the dominant behavior for $u \rightarrow -1$, or $\varphi \rightarrow 0$, i.e. for very early times. In this situation, it turns out that the terms containing the square roots are the dominant ones because they contain a pole. Then, neglecting the other terms, one can express the

variable u and, hence, the inflaton field vev φ in terms of the number of e-folds. This leads to

$$\varphi_{\text{IR}}(N) \simeq \varphi_{\text{ini}} \left[1 - \frac{\varphi_{\text{ini}}}{m_{\text{Pl}}} \sqrt{\frac{\alpha}{32\pi^2\beta}} N \right]^{-1}. \quad (149)$$

One checks that when the number of e-folds increases, the vev of the inflaton field increases. This clearly reproduces the behavior seen in Fig. 7. Notice that, in order to establish the previous formula, we have also assumed that $\varphi_{\text{ini}}/m_{\text{Pl}} \ll 1$ since $\varphi/m_{\text{Pl}} \ll 1$ and $\varphi_{\text{ini}} < \varphi$. Moreover, the approximation is valid only when the second term in the squared bracket of Eq. (149) is small in comparison to one such that the vev remains positive. When N is too large, the brane is far from the bottom of the throat and this approximation breaks down. Finally, in the previous section, we have established the constraint $\beta/\alpha \ll 1$. We see that, in Eq. (149), the inverse of this factor appears and in order to be consistent with the condition $\varphi/m_{\text{Pl}} \ll 1$, one must also have $\varphi_{\text{ini}}/m_{\text{Pl}} \ll \sqrt{\beta/\alpha}$.

Let us now turn to the UV case. In this situation, the variable u covers the range $u \in [1, +\infty[$ where the lower bound corresponds to $\varphi \rightarrow 0$. This is out of the canonical domain of definition for the elliptic integrals and to carry out the integration of Eq. (145), one can introduce the variable $1/u$. Moreover, the parameter n has now two disjoint ranges: for $0 < \alpha\beta^2 < 1$, $n \in]-\infty, 0[$, whereas for $\alpha\beta^2 > 1$ we get $n \in]1, +\infty[$. Some care is therefore required on the formulations of the elliptic integrals.

We first focus on the case where $\alpha\beta^2 > 1$. After appropriate redefinitions [57], the final trajectory reads

$$N_{\text{UV}}^{(n>1)}(\varphi) = 2\pi\beta \left[\frac{3n-1}{n} F\left(\arcsin \frac{1}{u} \middle| \frac{1}{n}\right) - \frac{3n-1}{n} F\left(\arcsin \frac{1}{u_{\text{ini}}} \middle| \frac{1}{n}\right) - 3E\left(\arcsin \frac{1}{u} \middle| \frac{1}{n}\right) + 3E\left(\arcsin \frac{1}{u_{\text{ini}}} \middle| \frac{1}{n}\right) \right. \\ \left. + 2 \ln \left(\frac{\sqrt{u_{\text{ini}}^2 - 1/n} + \sqrt{u_{\text{ini}}^2 - 1}}{\sqrt{u^2 - 1/n} + \sqrt{u^2 - 1}} \right) - \frac{(u-1)^2 - 4}{u} \sqrt{\frac{u^2 - 1/n}{u^2 - 1}} + \frac{(u_{\text{ini}}-1)^2 - 4}{u_{\text{ini}}} \sqrt{\frac{u_{\text{ini}}^2 - 1/n}{u_{\text{ini}}^2 - 1}} \right]. \quad (150)$$

At the end of inflation, i.e. when $\varphi \rightarrow 0$ (or $u \rightarrow 1$), the next term to last in Eq. (150) dominates, and we can

invert the resulting expression to obtain

$$\frac{\varphi_{\text{UV}}(N)}{m_{\text{Pl}}} \simeq \sqrt{\frac{32\pi^2\beta}{\alpha}} \frac{1}{N}. \quad (151)$$

Let us notice that, this time, the factor $\sqrt{\beta/\alpha} \ll 1$ directly appears in the above expression and, therefore, guarantees the consistency of the formula expressing the quantity $\varphi/m_{\text{Pl}} \ll 1$.

Let us now consider the case $0 < \alpha\beta^2 < 1$. The ellip-

tic integrals $F(\theta|p)$, $E(\theta|p)$ that arise in the calculation of Eq. (145) have now to be redefined for complex arguments θ and/or negative parameters p , respectively. After some calculations [57], the trajectory reads

$$\begin{aligned} \frac{N_{\text{UV}}^{(n<0)}(\varphi)}{2\pi\beta} = & \sqrt{1 + \frac{1}{|n|}} \left[F\left(\arcsin \sqrt{\frac{1+1/|n|}{u^2+1/|n|}} \middle| \frac{1}{|n|+1}\right) - F\left(\arcsin \sqrt{\frac{1+1/|n|}{u_{\text{ini}}^2+1/|n|}} \middle| \frac{1}{|n|+1}\right) \right. \\ & - E\left(\arcsin \sqrt{\frac{1+1/|n|}{u^2+1/|n|}} \middle| \frac{1}{|n|+1}\right) + E\left(\arcsin \sqrt{\frac{1+1/|n|}{u_{\text{ini}}^2+1/|n|}} \middle| \frac{1}{|n|+1}\right) \Big] \\ & + 2\sqrt{\frac{|n|}{|n|+1}} \left[-F\left(\arcsin \frac{\sqrt{u^2-1}}{u} \middle| \frac{1}{|n|+1}\right) + F\left(\arcsin \frac{\sqrt{u_{\text{ini}}^2-1}}{u_{\text{ini}}} \middle| \frac{1}{|n|+1}\right) \right. \\ & + E\left(\arcsin \frac{\sqrt{u^2-1}}{u} \middle| \frac{1}{|n|+1}\right) - E\left(\arcsin \frac{\sqrt{u_{\text{ini}}^2-1}}{u_{\text{ini}}} \middle| \frac{1}{|n|+1}\right) \Big] \\ & - 2\ln \left(\frac{\sqrt{u^2-1} + \sqrt{u^2+1/|n|}}{\sqrt{u_{\text{ini}}^2-1} + \sqrt{u_{\text{ini}}^2+1/|n|}} \right) - \frac{u^2(u-1)^2 - 4u^2 - 2(1+u)/|n|}{u\sqrt{(u^2-1)(u^2+1/|n|)}} \\ & + \frac{u_{\text{ini}}^2(u_{\text{ini}}-1)^2 - 4u_{\text{ini}}^2 - 2(1+u_{\text{ini}})/|n|}{u_{\text{ini}}\sqrt{(u_{\text{ini}}^2-1)(u_{\text{ini}}^2+1/|n|)}}. \end{aligned} \quad (152)$$

In the limit $u \rightarrow 1$ or $\varphi \rightarrow 0$, the next to last term in Eq. (152) dominates and we can approximately invert the above expression. The resulting trajectory ends up being given by the same expression as in Eq. (151). Finally, two typical UV trajectories are represented in Fig. 8.

Using these results, let us now turn to the observational predictions of these models. The Cosmic Background Explorer (COBE) normalization, implemented with the help of Eq. (125), leads to the following relation, valid for the UV and IR cases

$$\left(\frac{m_{\text{Pl}}}{\varphi_*}\right)^4 = \frac{45}{16\pi} \frac{Q^2}{T_{\text{cmb}}^2} \left(\frac{m_{\text{Pl}}}{m}\right)^2 \frac{\alpha}{\beta^2}. \quad (153)$$

This formula is only consistent when φ_*/m_{Pl} is a small quantity. In the limit $\varphi \rightarrow 0$, one has from Eq. (139) $\epsilon_1 \propto \varphi^3$ and

$$\delta_1 \underset{\varphi \rightarrow 0}{\sim} \frac{\varepsilon}{8\pi} \sqrt{\frac{2\alpha}{\beta}} \frac{\varphi}{m_{\text{Pl}}}, \quad \epsilon_2 \underset{\varphi \rightarrow 0}{\sim} -3\delta_1. \quad (154)$$

Therefore, ϵ_2 and δ_1 give the dominant contribution to the spectral index and one has

$$n_s - 1 \simeq 4\delta_1. \quad (155)$$

Using the COBE normalization given above leads to

$$n_s - 1 \simeq \varepsilon \left(\frac{16T_{\text{cmb}}^2}{15\pi^2 Q^2} \right)^{1/4} \lambda^{-1/4} \simeq 234.1\varepsilon \times \lambda^{-1/4}. \quad (156)$$

The spectral index only depends on the dimensionless 't Hooft coupling constant λ which is quite remarkable given the complexity of the equations and the number of free parameters of the model. In the UV case, the tilt is positive while it is negative in the IR case. In order to be compatible with the CMB data, one sees that one must have $\lambda \gtrsim 3 \times 10^{13}$.

The calculation of the running proceeds along the same lines. In the limit $\varphi \rightarrow 0$, one has

$$\delta_2 \underset{\varphi \rightarrow 0}{\sim} -\delta_1, \quad \epsilon_3 \underset{\varphi \rightarrow 0}{\sim} \frac{1}{3}(1-4\varepsilon)\delta_1. \quad (157)$$

Then, using Eq. (71), one obtains the following expression

$$\alpha_s \simeq -4\varepsilon\delta_1^2 = -\frac{\varepsilon}{4}(n_s - 1)^2. \quad (158)$$

The IR models ($\varepsilon = -1$) have therefore a red spectral index and a positive running while, on the contrary, the UV models ($\varepsilon = 1$) have a blue spectral index and a negative running. In Fig. 9, we have plotted the scalar power spectrum for the UV model stemming from an exact numerical integration of Eq. (24). Both the spectral index and the running match at a few percent with Eqs. (156) and (158).

One can also estimate the tensor to scalar contribution. For this purpose, one can compute the parameter $r = 16\epsilon_1/\gamma$, see Eq. (73). Using again the COBE nor-

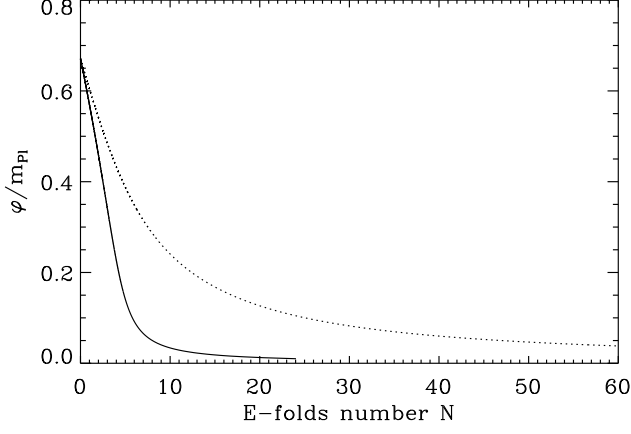


FIG. 8: Typical evolution of the scalar field φ according to Eq. (150) and Eq. (152) in the UV cases. The solid line refers the UV case with $n > 1$ since the parameters chosen are $\alpha = 404$ and $\beta = 0.05$ which implies $n = 101$. On the contrary, the dotted line represents a trajectory in the UV case with $n < 0$. The corresponding parameters are $\alpha = 4$, $\beta = 0.05$ which gives $n = -0.01$. In both cases, the initial condition is $\varphi_{\text{ini}}/m_{\text{Pl}} \simeq 0.67$.

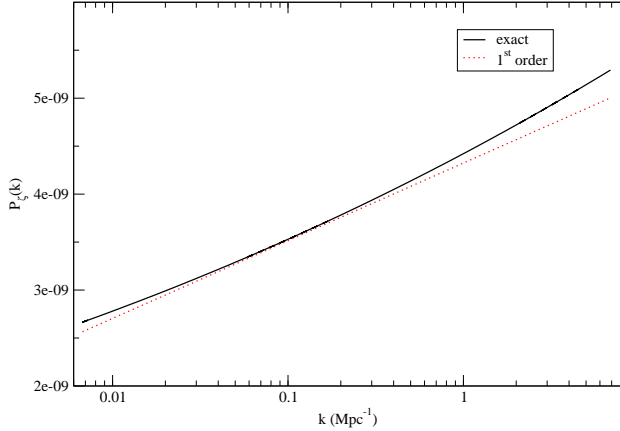


FIG. 9: Exact (solid) and first order (dotted) scalar power spectrum for the CKS plus constant UV models. The parameters are $\alpha = 38$, $\beta = 3.7$, $\lambda = 1.6 \times 10^{13}$ and $m^2 = 5 \times 10^{-4} m_{\text{Pl}}^2$. From the exact spectrum, one gets at the pivot $n_s - 1 \simeq 0.11$ and $\alpha_s \simeq -0.0023$ in agreement with Eqs. (156) and (158).

malization, straightforward manipulations lead to

$$r \simeq \frac{128\pi T_{\text{cmb}}^2}{15Q^2} \frac{\beta}{\alpha} \lambda^{-1}, \quad (159)$$

which is very small since $\beta/\alpha \ll 1$ and $\lambda^{-1} \propto (n_s - 1)^4$. Finally, the level of non-gaussianity can be estimated to

$$f_{\text{NL}} \simeq -\frac{35}{864} \sqrt{\frac{45}{\pi}} \frac{Q}{T_{\text{cmb}}} \frac{m_{\text{Pl}}/m}{\alpha^{1/2} \beta^2} \simeq -9.2 \times 10^{-7} \frac{m_{\text{Pl}}/m}{\alpha^{1/2} \beta^2}. \quad (160)$$

which is negative.

IV. CONCLUSION

In this section, we briefly recap and discuss the results obtained before. The main goal of our article was to present a generic formalism, as similar as possible to the standard approach, to investigate the features and the observational predictions of k-inflation. In particular, we have offered a new formula (but valid for DBI inflation only) for computing the classical trajectory for any warp function $T(\varphi)$ and potential $V(\varphi)$. Then, using the uniform approximation, we have computed the scalar and tensor power spectra, see Eqs. (53) and (57). These formulas are based on a double expansion. There is first an expansion around a pivot scale and, then, each coefficient of this expansion is in turn evaluated by means of another expansion, this time in terms of the Hubble and sound flow parameters. Finally, we have illustrated our results on various example models encountered in the literature. In particular, we have derived new results concerning the CKS models with constant term and obtained simple expressions for the cosmological observables.

Having generalized the standard formalism to k-inflation, the next step is of course to compare the predictions to the observations. This is done in Ref. [45] in the case of the CMB WMAP5 data.

Acknowledgments

LL acknowledges support through a DAAD PhD scholarship. This work is partially supported by the Belgian Federal Office for Science, Technical and Cultural Affairs, under the Inter-university Attraction Pole grant P6/11.

APPENDIX A: POTENTIAL AND WARP SLOW-ROLL PARAMETERS

In a broader sense, one can also try to establish another hierarchy of expansion parameters to the DBI case, namely in terms of the potential $V(\varphi)$ and the geometry parameter $T(\varphi)$. If we define the two parameters ϵ_v and ϵ_T according to

$$\epsilon_v \equiv \frac{1}{2\kappa} \left(\frac{V'}{V} \right)^2, \quad \epsilon_T \equiv \frac{1}{2\kappa} \left(\frac{T'}{T} \right)^2, \quad (A1)$$

where, in the present context, a prime means a derivative with respect to φ . We can establish the link with the (ϵ_i, δ_i) parameters. Straightforward manipulations lead to the following expressions

$$\epsilon_T = \frac{\gamma}{\gamma^2 - 1} \frac{\delta_1^2}{\epsilon_1}, \quad (A2)$$

$$\epsilon_v = \frac{\epsilon_1 \gamma}{4} \left[\frac{2(\gamma + 1) + \gamma(\delta_1 - \epsilon_2 - 2\epsilon_1)}{1 + \gamma(1 - \epsilon_1)} \right]^2. \quad (A3)$$

As can be expected, there is no one-to-one correspondence between the two sets of parameters (*i.e.*, for instance, the expression of ϵ_T not only involves ϵ_1 but also δ_1).

APPENDIX B: RELATIONS WITH OTHER SLOW-ROLL HIERARCHIES

In this Appendix, we briefly state the relations between our hierarchy of (ϵ_i, δ_i) parameters and the various parameter sets that have been used elsewhere in the literature. The parameters $(\epsilon_D, \eta_D, \kappa_D, \xi_D, \rho_D)$ defined in Ref. [35] can be expressed in terms of our parameters as follows:

$$\epsilon_D = \epsilon_1, \quad (B1)$$

$$\eta_D = \epsilon_1 - \frac{1}{2}(\epsilon_2 + \delta_1), \quad (B2)$$

$$\kappa_D = -\delta_1, \quad (B3)$$

$$\begin{aligned} \xi_D &= \frac{\epsilon_2 \epsilon_3}{2} + \frac{\delta_1 \epsilon_2}{2} - \frac{3}{2} \epsilon_1 \epsilon_2 \\ &+ \epsilon_1 \left(\epsilon_1 - \frac{3}{2} \delta_1 \right) + \frac{\delta_1}{2} (\delta_1 + \delta_2), \end{aligned} \quad (B4)$$

$$\rho_D = \frac{\delta_1}{2\epsilon_1} (2\delta_2 + 3\delta_1 - \epsilon_2). \quad (B5)$$

In Ref. [34], the first three of these parameters were used, changing the notation to $\epsilon_D \rightarrow \epsilon$ and so on. Then, it is interesting to compare the expression (2.30) of Ref. [35] to our Eq. (68). Written in terms of the Hubble and sound horizon parameters, this equation reads

$$\begin{aligned} n_s - 1 &= -2\epsilon_{1\Diamond} - \epsilon_{2\Diamond} + \delta_{1\Diamond} - 2\epsilon_{1\Diamond}^2 + (2D - 3)\epsilon_{1\Diamond}\epsilon_{2\Diamond} \\ &+ 3\epsilon_{1\Diamond}\delta_{1\Diamond} + \epsilon_{2\Diamond}\delta_{1\Diamond} + D\epsilon_{2\Diamond}\epsilon_{3\Diamond} - \delta_{1\Diamond}^2 \\ &+ 2D\delta_{1\Diamond}\delta_{2\Diamond}. \end{aligned} \quad (B6)$$

The claim made before can now be explicitly checked. The above formula coincides at first order with Eq. (68) but differs at second order. It is interesting to notice that the differences show up only in those terms containing the constant D .

A slightly different set of parameters $(\epsilon, s, \eta, \rho, {}^2\lambda)$ was recently introduced in Ref. [27], and expressed in terms of our (ϵ_i, δ_i) these parameters read

$$\epsilon = \epsilon_1, \quad (B7)$$

$$\eta = \epsilon_1 - \frac{1}{2}(\epsilon_2 + \delta_1), \quad (B8)$$

$$s = -\delta_1, \quad (B9)$$

$$\rho = \frac{\delta_1}{2\epsilon_1} (2\delta_2 + 3\delta_1 - \epsilon_2), \quad (B10)$$

$$\begin{aligned} {}^2\lambda &= \epsilon_1^2 + \frac{1}{2}(\epsilon_2 \epsilon_3 - 3\epsilon_1 \epsilon_2 + \epsilon_2 \delta_1 - 3\epsilon_1 \delta_1 \\ &+ \delta_1^2 + \delta_1 \delta_2). \end{aligned} \quad (B11)$$

Using this correspondance, one can explicitly check that Eq. (84) of Ref. [27] matches exactly with our Eq. (68),

the constant C in that reference being related to the constant D used in the present paper by $D = (C - 3)/4$. The small difference in the actual numerical values of $(C - 3)/4 = \ln 2 + \gamma_{\text{Euler}} - 7/4 \simeq -0.73$ and our $D = 1/3 - \ln 3 \simeq -0.76$ is the just the well-known difference between the WKB approximation versus the first order integration of the Bessel equation [43].

APPENDIX C: COSMOLOGICAL PERTURBATIONS FROM DBI INFLATION

In this Appendix, we briefly establish the conservation law for cosmological perturbations in k-inflation. This is important because as in the standard case [58], this allows us to propagate the primordial power spectra to the recombination epoch. We also briefly recall how the equation of motion for the Mukhanov-Sasaki variable can be obtained.

In the longitudinal gauge, the perturbed FLRW metric reads

$$\begin{aligned} ds^2 &= a^2(\eta) \{ - (1 + 2\Phi) d\eta^2 \\ &+ [(1 - 2\Psi) \delta_{ij} + h_{ij}] dx^i dx^j \}, \end{aligned} \quad (C1)$$

where Φ and Ψ are the Bardeen potentials which are coupled through the perturbed Einstein equation to the field perturbations $\delta\varphi$. The transverse and traceless tensor h_{ij} , *i.e.* satisfying $h_i{}^i = \partial^j h_{ij} = 0$ represents the spin two fluctuations which are not considered in the following since they are not affected by the DBI dynamics.

At the first order, the perturbed energy momentum tensor is obtained from Eq. (1) and its components read

$$\begin{aligned} \delta T^0_0 &= -\frac{\gamma^3}{a^2} \varphi' \delta\varphi' - \frac{dV}{d\varphi} \delta\varphi + \frac{(2 + \gamma)(\gamma - 1)^2}{2} \frac{dT}{d\varphi} \delta\varphi \\ &+ T\Phi\gamma(\gamma^2 - 1), \end{aligned} \quad (C2)$$

$$\delta T^k_0 = \frac{\gamma}{a^2} \varphi' \delta^{k\ell} \partial_\ell \delta\varphi, \quad (C3)$$

$$\begin{aligned} \delta T^k_\ell &= \left[\frac{\gamma}{a^2} \varphi' \delta\varphi' - \frac{dV}{d\varphi} \delta\varphi - \frac{(\gamma - 1)^2}{2\gamma} \frac{dT}{d\varphi} \delta\varphi \right. \\ &\left. - T\Phi \frac{\gamma^2 - 1}{\gamma} \right] \delta^k_\ell. \end{aligned} \quad (C4)$$

The gravitational sector remaining standard General Relativity whose perturbed Einstein tensor can be found in Ref. [59]. In particular, one still has the relation $\Psi = \Phi$ and there is only one degree of freedom because Φ and $\delta\varphi$ are related by the perturbed Einstein equations. One can therefore reduce the study of the scalar sector to the study of a single variable, as the comoving curvature perturbation

$$\zeta \equiv \Phi + \frac{\mathcal{H}}{\mathcal{H}^2 - \mathcal{H}'} (\Phi' + \mathcal{H}\Phi). \quad (C5)$$

From the background and perturbed equations, one can show that the comoving curvature perturbation can be

simplified to

$$\zeta = \Phi + \mathcal{H} \frac{\delta\varphi}{\varphi'}, \quad (\text{C6})$$

which also matches with its usual expression in standard inflation. Straightforward manipulations allows us to derive the expression of the derivative of ζ and one gets

$$\zeta' = -\frac{\mathcal{H}}{\mathcal{H}^2 - \mathcal{H}'} \frac{k^2}{\gamma^2} \Phi. \quad (\text{C7})$$

As a result, ζ is a conserved quantity on scales larger than the sonic horizon and allows us to propagate the spectrum from horizon exit till the beginning of the radiation dominated era. As usual, this result applies if the

decaying mode is neglected and in absence of entropy (isocurvature) perturbations [58].

The Mukhanov-Sasaki variable is now related to the comoving curvature perturbations by $v_{\mathbf{k}} = z\zeta$ where

$$z = \gamma^{3/2} \frac{a\varphi'}{\mathcal{H}}, \quad (\text{C8})$$

has a γ dependence. Using the previous equations, $v_{\mathbf{k}}$ is found to obeys the mode equation

$$v_{\mathbf{k}}'' + \left(\frac{k^2}{\gamma^2} - \frac{z''}{z} \right) v_{\mathbf{k}} = 0. \quad (\text{C9})$$

This is the equation already derived in Refs. [27, 34] and used in the text with the correspondence $c_s = 1/\gamma$.

-
- [1] B. Gold et al. (WMAP) (2008), 0803.0715.
 - [2] R. S. Hill et al. (WMAP) (2008), 0803.0570.
 - [3] G. Hinshaw et al. (WMAP) (2008), 0803.0732.
 - [4] M. R. Nolta et al. (WMAP) (2008), 0803.0593.
 - [5] J. Dunkley et al. (WMAP) (2008), 0803.0586.
 - [6] E. Komatsu et al. (WMAP) (2008), 0803.0547.
 - [7] E. D. Stewart and D. H. Lyth, Phys. Lett. **B302**, 171 (1993), gr-qc/9302019.
 - [8] J. Martin and D. J. Schwarz, Phys. Rev. **D62**, 103520 (2000), astro-ph/9911225.
 - [9] J. Martin, A. Riazuelo, and D. J. Schwarz, Astrophys. J. **543**, L99 (2000), astro-ph/0006392.
 - [10] D. J. Schwarz, C. A. Terrero-Escalante, and A. A. Garcia, Phys. Lett. **B517**, 243 (2001), astro-ph/0106020.
 - [11] S. M. Leach, A. R. Liddle, J. Martin, and D. J. Schwarz, Phys. Rev. **D66**, 023515 (2002), astro-ph/0202094.
 - [12] D. J. Schwarz and C. A. Terrero-Escalante, JCAP **0408**, 003 (2004), hep-ph/0403129.
 - [13] D. H. Lyth and A. Riotto, Phys. Rept. **314**, 1 (1999), hep-ph/9807278.
 - [14] J. M. Cline (2006), hep-th/0612129.
 - [15] R. Kallosh, Lect. Notes Phys. **738**, 119 (2008), hep-th/0702059.
 - [16] L. McAllister and E. Silverstein, Gen. Rel. Grav. **40**, 565 (2008), 0710.2951.
 - [17] C. Armendariz-Picon, T. Damour, and V. F. Mukhanov, Phys. Lett. **B458**, 209 (1999), hep-th/9904075.
 - [18] J. Garriga and V. F. Mukhanov, Phys. Lett. **B458**, 219 (1999), hep-th/9904176.
 - [19] S. Kachru et al., JCAP **0310**, 013 (2003), hep-th/0308055.
 - [20] M. Alishahiha, E. Silverstein, and D. Tong, Phys. Rev. **D70**, 123505 (2004), hep-th/0404084.
 - [21] G. R. Dvali and S. H. H. Tye, Phys. Lett. **B450**, 72 (1999), hep-ph/9812483.
 - [22] G. R. Dvali, Q. Shafi, and S. Solganik (2001), hep-th/0105203.
 - [23] S. H. S. Alexander, Phys. Rev. **D65**, 023507 (2001), hep-th/0105032.
 - [24] D. Baumann, A. Dymarsky, I. R. Klebanov, and L. McAllister, JCAP **0801**, 024 (2008), 0706.0360.
 - [25] D. Baumann, A. Dymarsky, I. R. Klebanov, L. McAllister, and P. J. Steinhardt, Phys. Rev. Lett. **99**, 141601 (2007), 0705.3837.
 - [26] X. Chen, M.-x. Huang, S. Kachru, and G. Shiu, JCAP **0701**, 002 (2007), hep-th/0605045.
 - [27] W. H. Kinney and K. Tzirakis, Phys. Rev. **D77**, 103517 (2008), 0712.2043.
 - [28] H. V. Peiris, D. Baumann, B. Friedman, and A. Cooray, Phys. Rev. **D76**, 103517 (2007), 0706.1240.
 - [29] S. Habib, K. Heitmann, G. Jungman, and C. Molina-Paris, Phys. Rev. Lett. **89**, 281301 (2002), astro-ph/0208443.
 - [30] S. Habib, A. Heinen, K. Heitmann, G. Jungman, and C. Molina-Paris, Phys. Rev. **D70**, 083507 (2004), astro-ph/0406134.
 - [31] M. Spalinski, JCAP **0705**, 017 (2007), hep-th/0702196.
 - [32] M. Spalinski, Phys. Lett. **B650**, 313 (2007), hep-th/0703248.
 - [33] I. R. Klebanov and M. J. Strassler, JHEP **08**, 052 (2000), hep-th/0007191.
 - [34] R. Bean, S. E. Shandera, S. H. Henry Tye, and J. Xu, JCAP **0705**, 004 (2007), hep-th/0702107.
 - [35] S. E. Shandera and S. H. H. Tye, JCAP **0605**, 007 (2006), hep-th/0601099.
 - [36] S. H. Henry Tye, Lect. Notes Phys. **737**, 949 (2008), hep-th/0610221.
 - [37] C. P. Burgess, PoS **P2GC**, 008 (2006), 0708.2865.
 - [38] J.-P. Bruneton and G. Esposito-Farese, Phys. Rev. **D76**, 124012 (2007), 0705.4043.
 - [39] E. Silverstein and D. Tong, Phys. Rev. **D70**, 103505 (2004), hep-th/0310221.
 - [40] L. Lorenz, J. Martin, and C. Ringeval, JCAP **0804**, 001 (2008), 0709.3758.
 - [41] R. Bean, D. J. H. Chung, and G. Geshnizjani (2008), 0801.0742.
 - [42] R. Bean, X. Chen, H. V. Peiris, and J. Xu, Phys. Rev. **D77**, 023527 (2008), 0710.1812.
 - [43] J. Martin and D. J. Schwarz, Phys. Rev. **D67**, 083512 (2003), astro-ph/0210090.
 - [44] R. Casadio, F. Finelli, M. Luzzi, and G. Venturi, Phys. Rev. **D71**, 043517 (2005), gr-qc/0410092.
 - [45] L. Lorenz, J. Martin, and C. Ringeval (2008), 0807.2414.
 - [46] M. Spalinski, JCAP **0804**, 002 (2008), 0711.4326.
 - [47] X. Chen, Phys. Rev. **D71**, 063506 (2005), hep-th/0408084.

- [48] X. Chen, JHEP **08**, 045 (2005), hep-th/0501184.
- [49] R. Bean, J. Dunkley, and E. Pierpaoli, Phys. Rev. **D74**, 063503 (2006), astro-ph/0606685.
- [50] X. Chen, S. Sarangi, S. H. Henry Tye, and J. Xu, JCAP **0611**, 015 (2006), hep-th/0608082.
- [51] D. A. Easson, R. Gregory, D. F. Mota, G. Tasinato, and I. Zavala, JCAP **0802**, 010 (2008), 0709.2666.
- [52] D. Easson, R. Gregory, G. Tasinato, and I. Zavala, JHEP **04**, 026 (2007), hep-th/0701252.
- [53] D. Baumann and L. McAllister, Phys. Rev. **D75**, 123508 (2007), hep-th/0610285.
- [54] J. Martin and C. Ringeval, JCAP **0608**, 009 (2006), astro-ph/0605367.
- [55] W. H. Kinney, E. W. Kolb, A. Melchiorri, and A. Riotto, Phys. Rev. **D74**, 023502 (2006), astro-ph/0605338.
- [56] D. Seery and J. E. Lidsey, JCAP **0506**, 003 (2005), astro-ph/0503692.
- [57] M. Abramowitz and I. A. Stegun, *Handbook of mathematical functions with formulas, graphs, and mathematical tables* (National Bureau of Standards, Washington, US, 1970), ninth ed.
- [58] J. Martin and D. J. Schwarz, Phys. Rev. **D57**, 3302 (1998), gr-qc/9704049.
- [59] V. F. Mukhanov, H. A. Feldman, and R. H. Brandenberger, Phys. Rept. **215**, 203 (1992).